AD_____

AWARD NUMBER: W81XWH-04-1-0157

TITLE: Targeting Stromal Recruitment by Prostate Cancer Cells

PRINCIPAL INVESTIGATOR: Jingxian Zhang, Ph.D.

CONTRACTING ORGANIZATION: University of Wisconsin
Madison, Wisconsin 53706-1490

REPORT DATE: March 2006

TYPE OF REPORT: Annual Summary

PREPARED FOR: U.S. Army Medical Research and Materiel Command
Fort Detrick, Maryland 21702-5012

REPORT DOCUMENTATION PAGE

Form Approved
OMB No. 0704-0188

1. REPORT DATE *(DD-MM-YYYY)*	**2. REPORT TYPE**	**3. DATES COVERED** *(From - To)*
01-03-2006	Annual Summary	15 Feb 2004 – 14 Feb 2006

4. TITLE AND SUBTITLE

Targeting Stromal Recruitment by Prostate Cancer Cells

5a. CONTRACT NUMBER

5b. GRANT NUMBER
W81XWH-04-1-0157

5c. PROGRAM ELEMENT NUMBER

6. AUTHOR(S)

Jingxian Zhang, Ph.D.

E-Mail: zhangj@surgery.wisc.edu

5d. PROJECT NUMBER

5e. TASK NUMBER

5f. WORK UNIT NUMBER

7. PERFORMING ORGANIZATION NAME(S) AND ADDRESS(ES)

University of Wisconsin
Madison, Wisconsin 53706-1490

8. PERFORMING ORGANIZATION REPORT NUMBER

9. SPONSORING / MONITORING AGENCY NAME(S) AND ADDRESS(ES)
U.S. Army Medical Research and Materiel Command
Fort Detrick, Maryland 21702-5012

10. SPONSOR/MONITOR'S ACRONYM(S)

11. SPONSOR/MONITOR'S REPORT NUMBER(S)

12. DISTRIBUTION / AVAILABILITY STATEMENT
Approved for Public Release; Distribution Unlimited

13. SUPPLEMENTARY NOTES

14. ABSTRACT

Sonic hedgehog(shh)overexpression in LNCaP cells accelerates tumor growth. To characterize the contributions of each Gli gene to Shh-induced tumor growth, Gli1, Gli2 and Gli3 knockout UGSM cells have been isolated and UGSM-2 cells independently over-expressing hGli1 and hGli2 were cloned. Experiments using those cell lines co-injected with LNCaP cells in the Xenograft model indicate stromal Shh signaling activation may play an important role in the tumor growth.

15. SUBJECT TERMS
prostate cancer, tumor, sonic hedgehog signal,Gli

16. SECURITY CLASSIFICATION OF:			**17. LIMITATION OF ABSTRACT**	**18. NUMBER OF PAGES**	**19a. NAME OF RESPONSIBLE PERSON**
a. REPORT	**b. ABSTRACT**	**c. THIS PAGE**			USAMRMC
U	U	U	UU	54	**19b. TELEPHONE NUMBER** *(include area code)*

Table of Contents

Introduction:

Hedgehog (hh) is secreted glycopeptides that act as potent inducers of morphogenesis and growth in a variety of tissues and structures during embryogenesis, including limb, brain, eye, and lung development. There are three hedgehog ligands, sonic hedgehog (Shh), indian hedgehog (Ihh), and desert hedgehog (Dhh). As summarized in Figure 1, Shh is secreted and binds to a specific receptor Patched (Ptc) on the target cell surface. Shh binding to Patched leads to the release of Smoothened, a protein which also associates with Patched. The release of Smoothened activates an intracellular signal transduction pathway and ultimately Gli gene activation. Three Gli genes (Gli1, Gli2, and Gli3) encode transcriptional regulators which share a conserved DNA-binding domain and bind the same recognition sequence. Gli1 acts as a transcriptional activator, and Gli2 is believed to be largely redundant in function with Gli1. In contrast, Gli3 is believed to function as both an activator and repressor of transcription, with most Gli3 effects being mediated through its repressor function. Gli1 and Ptc are primary targets of Hh pathway activation and serve as reliable indicators of Hh signaling.

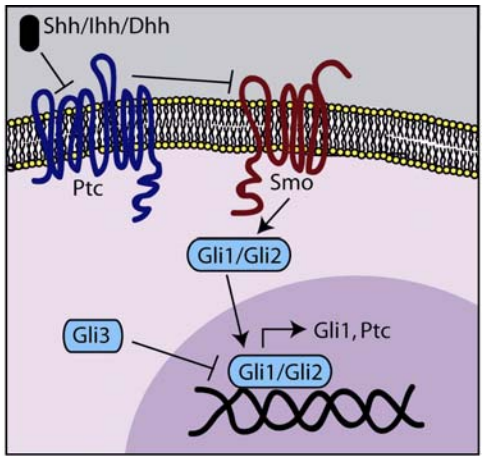

Figure 1. The mammalian Hh signaling pathway[5]. Hedgehog ligand bind to the transmembrane receptor Patched (Ptc) and relieve repression of Smoothened (Smo). Smo activation curtails transcriptional repression by Gli3 and promotes activation/translocation of Gli1 and Gli2 to the nucleus, resulting in transcriptional activation of Hedgehog target genes.

Hedgehog signaling is a key regulator of normal prostate development. Hh ligand is expressed by the epithelial cells of the developing prostate and exerts a combination of autocrine and paracrine signaling activities to

stimulate cell proliferation and ductal morphogenesis. Studies of Hh in normal and neoplastic human prostate demonstrated comparable levels of expression of Hh ligand and Gli1 in specimens of benign and localized prostate cancer, with a suggestion of higher level expression in locally advanced and androgen independent prostate cancer. Shh expresses in the tumor epithelium with localization of Gli1 predominantly in the peri-glandular tumor stroma.

Previous work in Dr.Bushman lab[1] using LNCaP xenograft model shown that (1) shh expression by LNCaP prostate tumor cells activates Gli gene expression in adjacent tumor stroma. (2) genetically engineered shh over-expression in LNCaP cells leads to increased tumor stromal Gli-1 expression but the hGli1 expression of LNCaP cell didn't change, and (3) shh over-expression dramatically accelerates tumor growth . Activation stroma-mediated paracrine signals by epithelial sonic hedgehog expression to promote tumor growth was then demonstrated. To test the hypothesis that activation of stromal Gli gene expression is sufficient to promote tumor growth and elucidate the roles of the three different Gli genes in the stromal response to Shh signaling, we planned to examine the effects of gain and loss function of Gli gene using a xenograft tumor model in which LNCaP cells are co-injected with cloned, immortalized stromal cells. The value of this tumor model is that it would provide us with the opportunity to selectively assay gene expression in the stromal and epithelial compartments of the tumor using species specific PCR primers and to make specific modifications in stromal cell gene expression.

Body

Material and Method:

Cell Lines. All the prostate cancer cell lines were purchased from American Type Culture Collection (ATCC, Manassas, VA) and maintained in the medium recommended by ATCC. BPH1 cells were a generous gift from Dr. Simon Hayward (Vanderbilt University, Nashville, TN) and were grown in RPMI 1640 medium plus 5% fetal calf serum (FCS). Four cDNA samples from independent human prostate epithelial cultures were kindly provided by Dr. David Jarrard (University of Wisconsin, Madison, WI). Human prostate total RNA and fetal brain total RNA were purchased from BD Biosciences (Palo Alto, CA). Human prostate total RNA was pooled from normal prostates of 32 Caucasian males ages 21-50. Human fetal brain total RNA is from normal fetal brains pooled from 21 spontaneously aborted male/female Caucasian fetuses, ages 26-40 weeks. Cells were plated in a 24-

well plate at a density of 1×10^5 cells/well. RNA was harvested after 3 days for the comparison of Hh pathway gene expression in different cell lines. For the assay of gene expression after SHH/cyclopamine treatment, serum concentration was reduced to 1% after 1 day attachment, and either 1nM, 10nM octylated N-Shh (Curis, Inc., Cambridge, MA) or 5uM cyclopamine (Toronto Research chemicals, Ontario, Canada) was added to the medium and RNA was harvested after 48 hours treatment. Shh doses of 1nM and 10nM were selected based on efficacy in Gli-luciferase assay (Figure 3). A 1nM dose of octylated N-Shh equates with a 400nM dose of unmodified N-Shh. Each experiment was repeated three times independently. UGSM-2 cells[6] and MEFs were isolated in our laboratory.

Molecular cloning. Vectors PLTR-Gli1, pCMV-Gli2 and pDZ77-Gli3 were kindly provided by Dr.Iannaccone. Restriction sites for cloning of cDNAs into suitable vecotors will be introduced through PCR using oligonucleotide primers which contain suitable restriction sites. PCR products will be digested, purified and ligated into the appropriate vector. Ligation mixtures will be used to trandform *E.coli* and clones will be identified through plasmid isolation, followed by restriction digest, gel electrophoretic analyses and sequencing.

RNA isolation and real time RT-PCR. RNA was isolated using Qiagen (Valencia, CA) RNeasy RNA isolation Kits and subjected to on-column DNase digestion. cDNA was generated following standard protocols. Gene expression was assayed by real time RT-PCR using SYBR Green PCR Master Mix (Applied Biosystems, Foster City, CA) on BioRad iCycler instrument (Hercules, CA) and using glyceraldehyde-3-phosphate dehydrogenase (GAPDH) as an internal standard gene.

Isolation of Gli knock out UGSM cells. Heterozygous $Gli1^{(+/-)}$, $Gli2^{(+/-)}$ and $Gli3^{(+/-)}$ mice (INK4A homozygous background) were bred to generate $Gli1^{(-/-)}$, $Gli2^{(-/-)}$ and $Gli3^{(-/-)}$knockout embryos. Male mouse embryos were harvested at 16 days post-conception and the prostate mesenchymal cell layer were isolated by trysin and collagenase digestion to recover single cells. These cells were grown in culture where they spontaneously immortalize due to the INK4A (P16, P19 knock out) background. Cell lines have been characterized by quantitative real time PCR.

.

Adenovirus infection. Adenovirus constructs carrying ΔNmGli2-GFP, hSmo*-GFP or GFP alone were kindly provided by Dr. Chen-Ming Fan

(Carnegie Inst, Baltimore, MD). Cells were plated in a 24-well plate at density of 1×10^5 cells/well. After 24 hours attachment, media was replaced with 1% FCS +/- adenovirus at a multiplicity of infection of 25-100 PFU/cell. Sonic hedgehog and cyclopamine were added at the same time. RNA was harvested and gene expression was determined as described below. Under these conditions, more than 90% of cells were infected according to GFP fluorescence analysis by flow cytometry.

Retrovirus infecton. VSV-G pseudotyped murine leukemia virus expressing EGFP was generously provided by F. Michael Hoffmann. UGSM-2 cells in culture were infected with retrovirus carrying different Gli gene for 3 hours and GFP expressing cells were collected by FACS analysis 1 week later. Tissues were processed and stained for GFP using the immunohistochemistry procedure described blow.

Xenografts. Xenograft tumors were generated in adult male CD-1 nude mice. $2x10^6$ LNCaP cells were mixed with $0.5x10^6$ INK4 cells and 50% Matrigel and injected subcutaneously on the flanks of mice. Tumors were measured weekly with calipers and tumor volume was calculated as the volume of a spheroid using the formula: Vol = LxWxHx0.5236.

GFP immunohistochemistry. Formalin-fixed paraffin embedded sections were dewaxed, rehydrated and processed for antigen retrieval. Sections were blocked with 1% BSA + 10% normal goat serum in PBS for 1 hour and then incubated overnight at 4°C with rabbit anti-GFP (Chemicon, Temecula, CA) diluted to 4 ug/ml in block solution. Anti-GFP was visualized by incubation with 5 ug/ml goat anti-rabbit-Alexa 488 conjugate (Molecular Probes, Eugene, OR) for 45 minutes at room temperature. Slides were mounted with Vectashield Hardset + DAPI mounting media (Vector, Burlingame, CA) and imaged using an Olympus model BX51 fluorescent microscope and Spot Advanced software v. 3.5.2.

Statistics. We analyzed tumor growth rate by obtaining slopes. These were obtained by calculating the difference between final and initial tumor volumes, and then dividing by the intervening number of weeks: $(V_n - V_0)/n$, where V_0 denotes the tumor volume (in mm^3) when it first becomes apparent, V_n denotes the tumor volume n weeks later, and n is the number of weeks between tumor appearance and the end of the experiment or the week in which the animal needed to be euthanized, whichever occurred earlier. Tumors with one or more of the following conditions were excluded from

the analysis: those with a final volume of less than $100mm^3$, those that contracted (i.e. final volume < initial volume), those that were undetectable in any given week post initial establishment, and those with a slope less than $10mm^3$/week. One-Way Analysis of Variance (ANOVA) was used to test for differences in growth rate (slope) due to treatment; slopes within a given animal were considered independent. If the overall *F*-test was significant ($P < 0.05$) pair-wise comparisons between treatments were examined. This procedure is equivalent to Fisher's protected least-squares differences (LSD). In order to better meet the assumptions of ANOVA, rank and logarithmic transformations of the original data were considered. Slopes for tumor growth seemed to have a slightly positive skew distribution. A logarithmic transformation did not improve matters, so ANOVA was performed on the raw slopes. We analyzed differences in gene expression by comparing the average GAPDH normalized value for each gene using a *t*-test assuming unequal variances.

Results:

Generation of UGSM-2 cells stably over-expressing Gli1 or Gli2. In order to examine the effect of stromal Gli gene over-expression on xenograft tumor growth, we need to creat postate stromal cells stably over-expressing Gli1 or Gli2, then we can coinject them with LNCaP prostate cancer cells to characterize the influence of each Gli gene on tumor growth.

Cloned, immortalized UGS (Urogenital Sinus) mesenchymal cell line (UGSM-2) has been derived from the E16 UGS of the INK4 mouse, a transgenic knockout that lacks both p16 and p19[6]. These cells respond to shh treatment in culture, do not form tumors in nude mice when co-injected alone with matrigel, and do form tumors in nude mice when co-injected with LNCaP cells and matrigel.

We had encountered unexpected difficulties in generating stably over-expressing Gli1 or Gli2 UGSM-2 cells. As proposed, I first chose the expression vector pCDNA3.1/Hygro(+), and inserted the coding sequence of human Gli1 gene into the Vector. UGSM-2 cells were then transfected with pCDNA-Gli1 DNA using Lipofectomine 2000, at the same time, cells was transfected with pCDNA3.1/Hygro(+) as control. 200ug/ml hygromycin were added into the medium as the selection marker. Quantitative real time PCR results were shown in Figure2A, in the UGSM-2 cells over-expressing Gli1, the expression level of mGli1 gene is about 18 fold higher, mPatched gene is 3.6 fold higher. But under hygromycin selection, the UGSM-2 cells changed their morphology, they became much smaller than the normal cells

without antibiotics selection and Gli1 can't be stably over-expressed in the mixed cells (data not shown).

Then the basal expression vector was changed to pIRES-EGFP, so we can use flow cytometry to sort the cells with Gli based on the co-expressed green fluorescence protein of the transfected cells. The coding sequence of Human Gli2ß gene was inserted to pIRES-EGFP. Two days after transfection, cells were trypsinized and isolated by sterile cell sorting on a FACs Vantage SE cell sorter equipped with FACS Diva Option software. Figure 2B shows that mGli2 gene is over-expressed (19 fold higher than the control) in the cells and the expression of mPatched gene were also induced. But the Gli2 gene still can not stably over-expressed in the mixed cell population, the cells lost gli2 over-expression after several passages in vitro (data not shown).

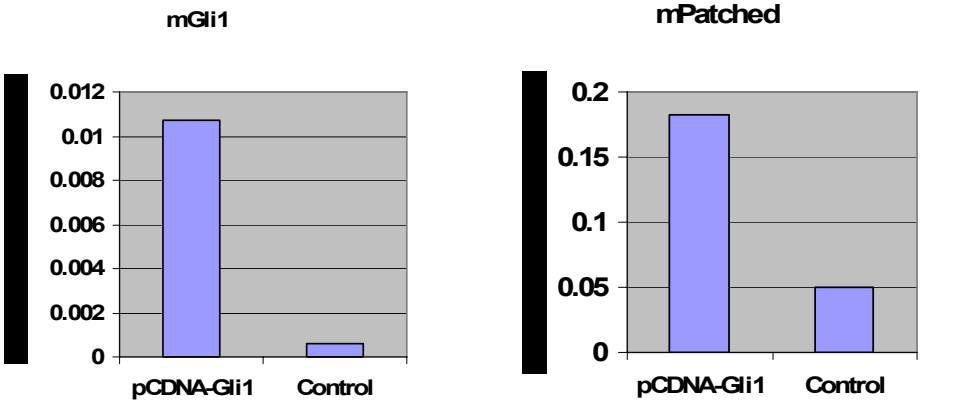

A

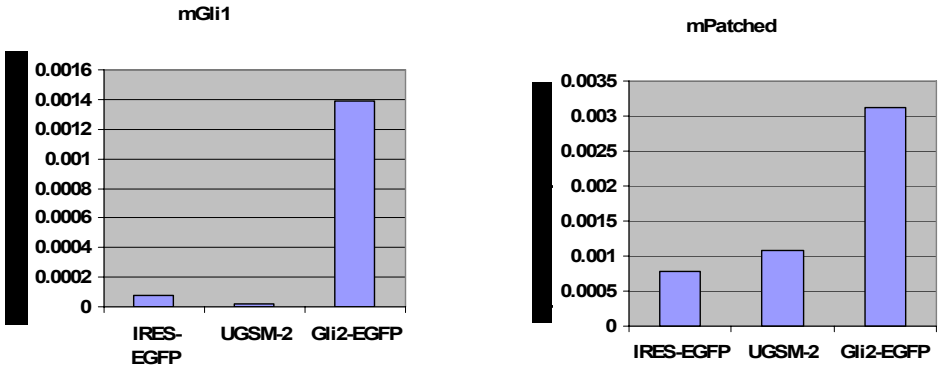

B

Figure 2. Real time PCR shows over-expression of human Gli1 and Gli2 gene in the mouse UGSM-2 cells. Mouse Gli1 was over-expressed in UGSM-2 cells transfected with pCDNA-Gli1 and downstream target genes Patched was also activated (Figure2A). Mouse Gli1, Patched were over-expressed in the UGSM cells over-expressing Gli2 (Figure 2B), cells transfected with pIRES-EGFP was a control.

Since UGSM-2 cells can't stably over-express Gli1 or Gli2 after DNA transfection, the genes were cloned into a retrovirus vector (pRetro-IRES-GFP) seperately. UGSM-2 cells were infected with retrovirus carrying human Gli or Gli2, single cell lines that stably over-express hGli1 or hGli2 were isolated after sorting. As shown in Figure 3A, clones Gli1.1 and Gli1.2 isolated from infected UGSM-2 cells by retrovirus carrying hGli1 gene over-express mGli1 and mPtc, the expression level did not change after 1 month growing in culture (data not shown). Out of 24 clones from UGSM-2 cells infected by retrovirus carrying hGli2 protein, clone 9 was selected in which cells stably over-express hGli2, mPatched and mGli1 (Figure3B), so cell lines stably over-expressing Gli1 or Gli2 were established.

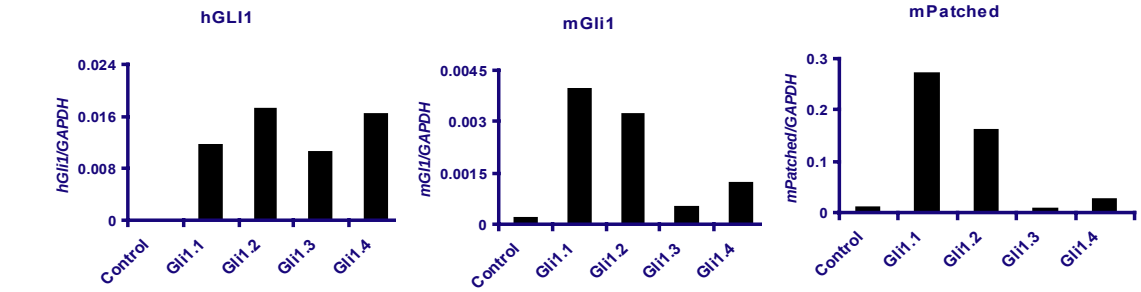

A

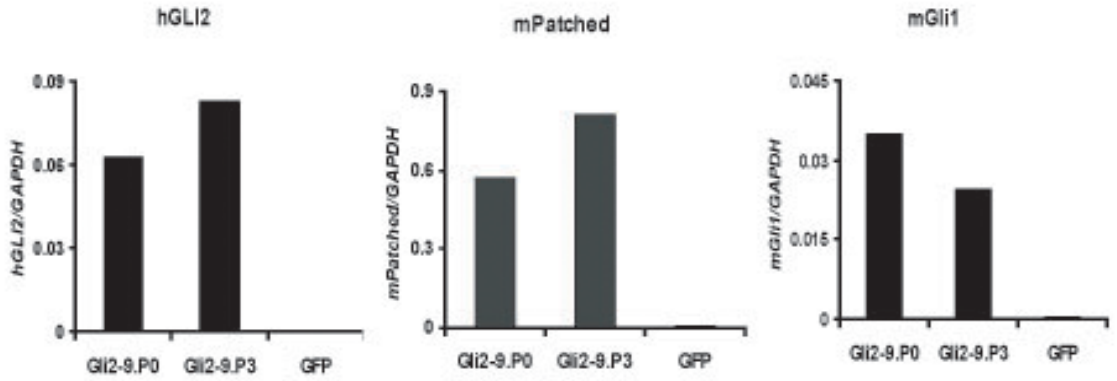

B

Figure 3. QRT-PCR analysis of different single clones over-expressing hGli1 (Figure 3A) or hGli2 (Figure 3B). UGSM-2 cells over-expressing GFP works as control, CDNA from different clones were assayed by QRT-PCR. Downstream target gene mGli1 and mPatched are highly activated in clones Gli1.1 or Gli1.2 over-expressing hGli1, and Gli2-9 over-expressing hGli2. Gli2-9. P0, passage 0 of Gli2-9, Gli2-9.P3: passage 3 of Gli2-9.

Effects of Gli over-expressing UGSM-2 cells on Xenograft tumor formation. For testing the activation of stromal Gli1 or Gli2 is sufficient to promote tumor growth, we co-injected the LNCaP cells and UGSM-2 cells over-expressing Gli1(Gli1.1) or Gli2 (Gli2-9) into nude mice and measured the tumor growth, using UGSM-2 cells infected with retrovirus only carrying pRetro-IRES-GFP as control. We couldn't detect any difference of UGSM-GFP and UGSM-Gli1 on tumor growth (Figure 4A), and real time PCR results show that none of the Gli1 gene (hGli1 or mGli1) were activated in the LNCaP+UGSM-Gli1 tumor samples (Figure 4B). This may due to cells having lost Gli1 activation in vivo or that cells over-expressing Gli1 were diluted out during tumor growth.

HGli2 over-expression in UGSM-2 cells was able to induce morphological transformation in culture (Figure4C). When those cells co-injected with LNCaP cells into the nude mice, tumors grow faster than control (data not shown). However, immunohistochemical staining showed that tumors are mainly composed of GFP positive UGSM-2 cells, indicating that the tumors containing UGSM-2 cells over-expressing GLi2 are sarcomas (Figure4D).

Generation of Gli1, Gli2 and Gli3 –null UGSM cell lines. In order to examine the effect of Gli1, Gli2 , and Gli3 loss on xenograft tumor growth, Gli1, Gli2 and Gli3 knockout UGSM cells were islolated respectively.

$Gli1^{(-/-)}$, $Gli2^{(-/-)}$ and $Gli3^{(-/-)}$ knockout cells were treated with shh and cyclopamine (shh pathway inhibitor). Quantitative real time PCR results confirmed that these knockout cells still respond to shh and cyclopamine, exogenous shh can activate gene expression of gli1 and patched, and cyclopamine can block the activation (Figure 5, 6 and 7).

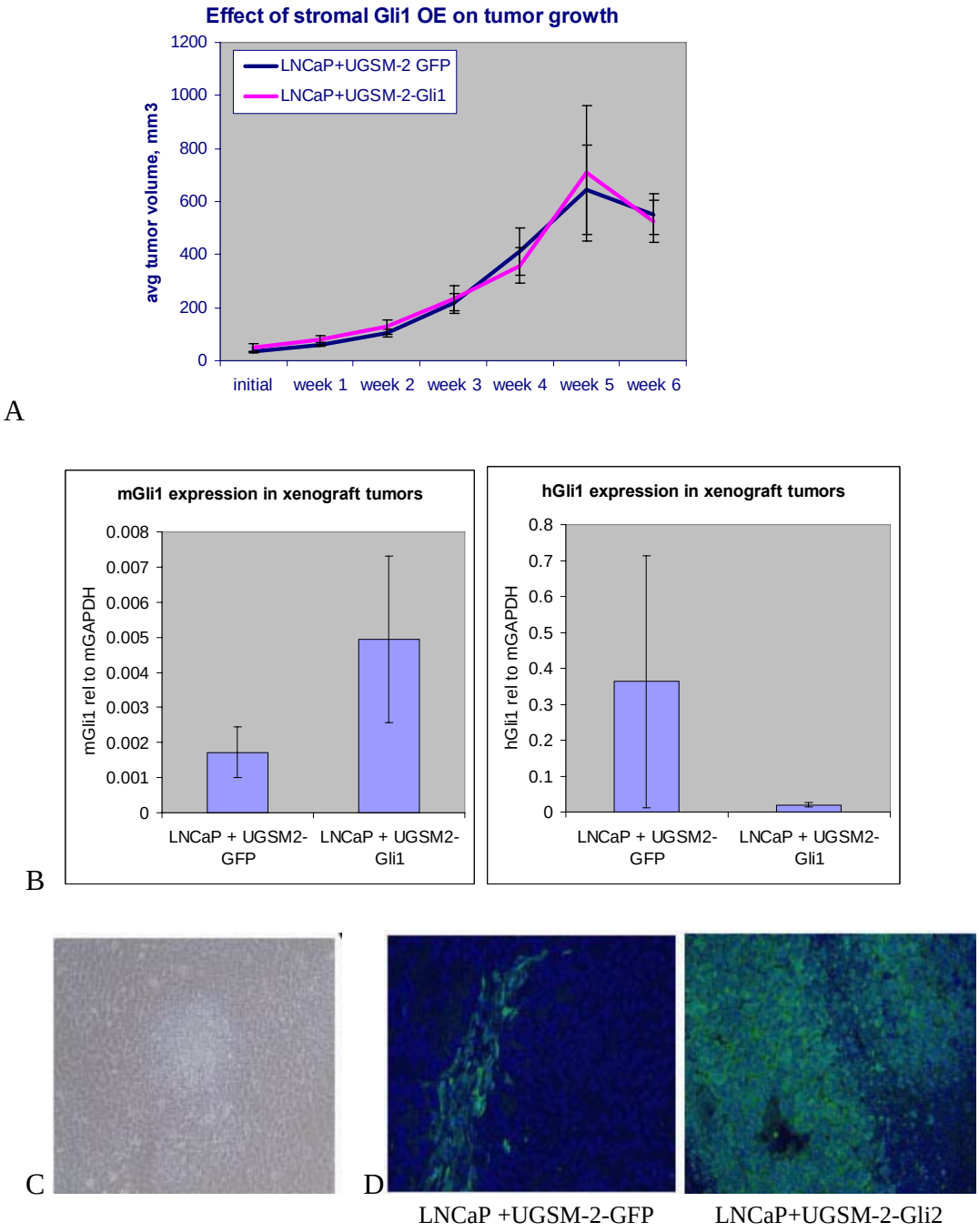

Figure 4. Effect of stromal Gli over-expressing on tumor growth. The growth of LNCaP + UGSM-2-Gli1 tumor didn't show any difference compared to control (Figure3A), P>0.05. Neither hGli1 or mGli1 was over-expressed in the xenograft tumors (Figure 3B), P>0.05. For each group, data were analyzed from the real time PCR results from three different tumors. (C) Over-expression of Gli2 caused cell transformation. (D) Immunohistochemical staining for GFP positive UGSM-2 cells in the xenograft tumor. Left is control tumor (LNCaP+UGSM-2 GFP), Right is UGSM-2 over-expressing Gli2 cells co-injected with LNCaP. Compared to control, LNCaP+ UGSM-2-Gli2 tumors are mainly composed of UGSM-2 cells (green cells), indicating the tumors are sarcomas. Blue is for DAPI, Green is for GFP.

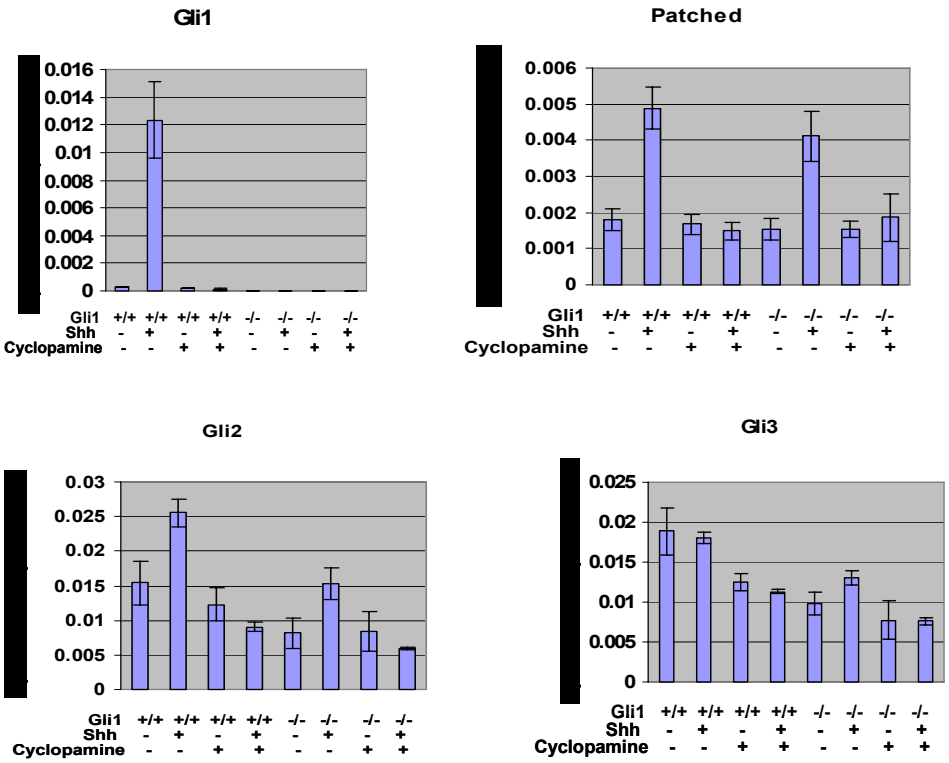

Figure 5. The response of Gli1$^{(-/-)}$ knockout cells to shh and cyclopamine. Cells were treated with 1nM shh and 5μM cyclopamine. The gene expression level was all compared to GAPDH. No gli1 expression was detected in the knockout cells. The expression of gli2 and gli3 are similar in the knockout cells compared to wild type cells.

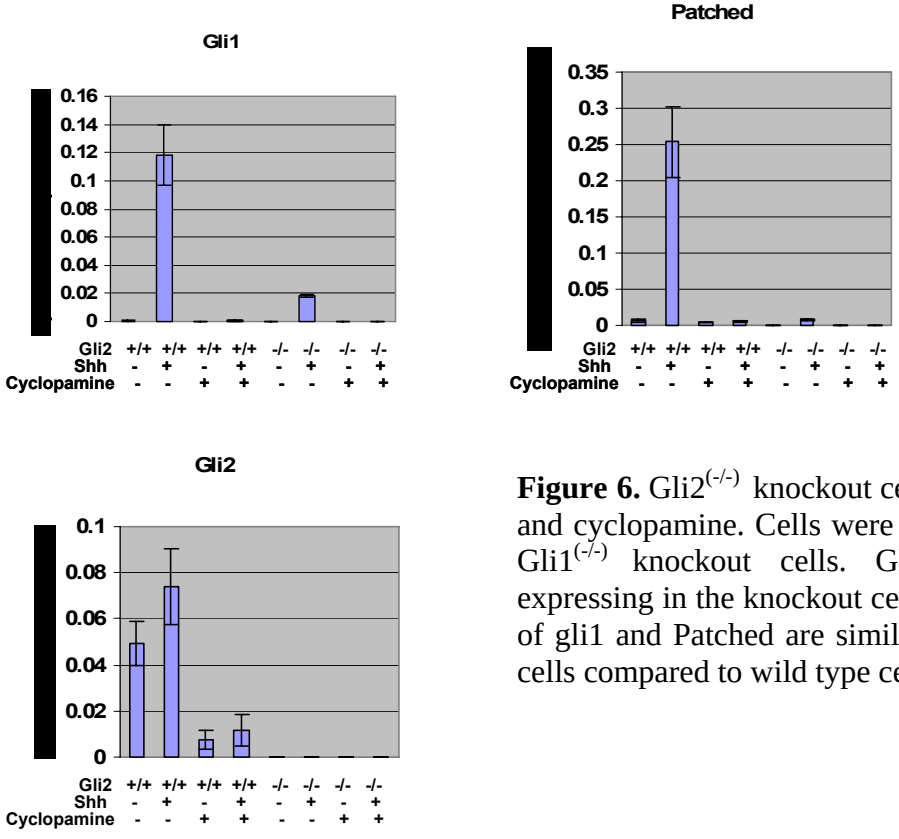

Figure 6. Gli2$^{(-/-)}$ knockout cells respond to shh and cyclopamine. Cells were treated as same as Gli1$^{(-/-)}$ knockout cells. Gli2 gene is not expressing in the knockout cells. The expression of gli1 and Patched are similar in the knockout cells compared to wild type cells.

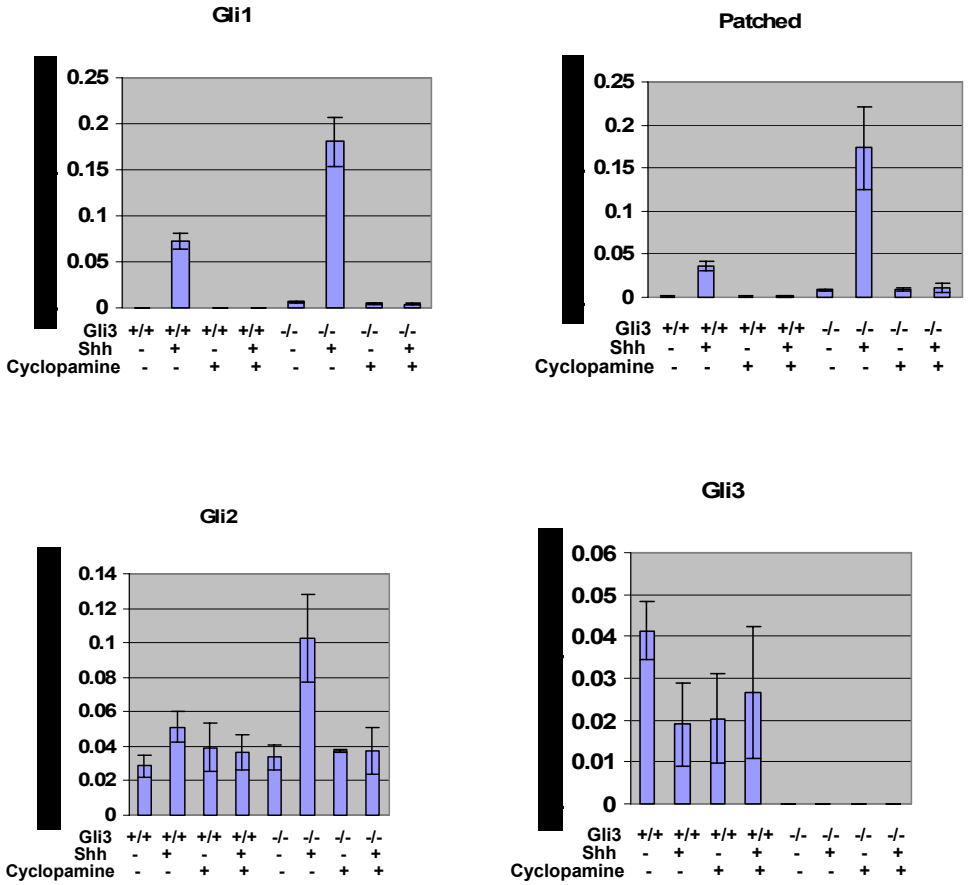

Figure 7. The response of Gli3$^{(-/-)}$ knockout cells to shh and cyclopamine. Cells were treated as before. Gli3 expression was not detected in the knockout cells. The expression of gli1 and patched are about 2-3 fold higher in the knockout cells, it means that gli3 works as a negative regulator in the shh pathway of mouse UGSM cells.

Effects of Gli knock out UGSM-2 cells on Xenograft tumor formation

The proposed experiments were to identify which Gli gene is critical for shh-induces tumor growth in the LNCaP xenograft model. We expected that deletion of one of the Gli genes in UGSM-2 cells would lead to no increase in tumor growth when this UGSM-2 cell line was co-injected with LNCaP cells which over-express Shh, as the critical downstream Shh target Gli gene would be disrupted. Preliminary studies in our lab show that at least 50% stromal cells from the LNCaP+ UGSM-2-GFP xenograft tumors are host stromal cells, so the Gli genes in the host stromal cells will still exist and respond to shh, it may be impossible to knock out any Gli gene in the tumor stroma. We will perform additional unfunded studies to determine whether co-injection of Gli2 knock out cells significantly decrease stromal Hh pathway activity. If not, the experiments using Gli1 or Gli2 knock out

stromal cells co-injected with LNCaP or LNCaP over-expressing shh will not be pursued.

Gli3 is thought to function primarily as a transcriptional repressor, the knock out cells have activated shh signaling (higher expression of mGli1 and mHip as indicated by QRT-PCR, Figure 7). Even there are host stormal cells, the stromal mGli1 and mHip gene should still activate compared to control. As we expected, co-injection of Gli3 null stromal cells resulted in rapid growth of tumors when compared with tumors containing wild-type stromal cells (Figure 8).

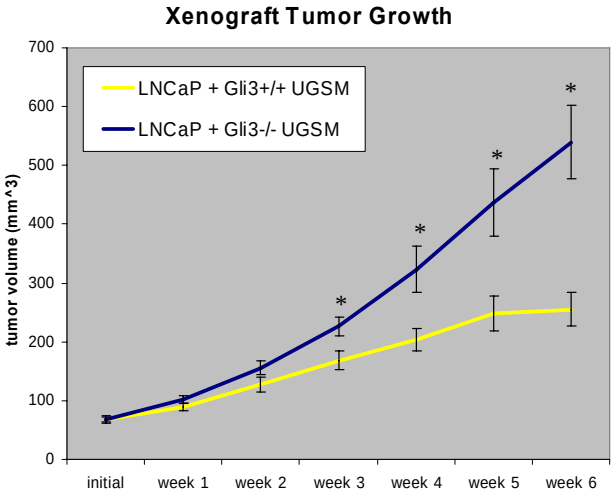

Figure8. Accelerated growth of LNCaP + Gli3-/- Xenograft relative to LNCaP + Gli3+/+ xenograft. *significantly different from Gli3+/+ at time indicated, $p<0.01$.

Autocrine Hh signaling is not involved in growth of human prostate cancer cells. As mentioned above, activation shh downstream target gene in Gli3 knock out cells can promote tumor growth and previous work in our lab has shown that shh over-expression in LNCaP cells dramatically accelerates tumor growth, leading to increased tumor stromal Gli-1 expression but not hGli1 expression of LNCaP cell. However, other studies[2,3,7] suggest that autocrine Hh signaling may contribute to tumor growth, we wished to test whether autocrine hh signaling is also involved in the prostate cancer cell growth.

Detailed analysis of Hh signaling in prostate cancer cells revealed that LNCaP, PC3, 22RV1 cells do not respond to Shh by increasing expression of the canonical Hh signaling mediators Gli1 and Ptc1 (Figure 9). In fact, expression of Smo in 22RV1, PC-3 cells or LNCaP cells does not induce pathway activation as it does in other shh-responsive cell lines (Figure 10). However, expression of Gli1 or Gli2 in 22RV1 or PC-3 cells does induce transcription of Hh target genes Gli1 and Ptc (Figure 11). These studies revealed that intracellular Hh signal transduction in normally used prostate

cancer cells is functionally impaired and pathway target genes can only be induced by expression of the final mediators of the Hh transcriptional response. We have recently found that Hh signaling is similarly impaired in LNCaP and PC3 tumor (data not shown), lending credence to the idea that those cancer cells are not capable of Hh signal transduction and growth effects on tumors must be mediated by paracrine interactions with other cells in the tumor.

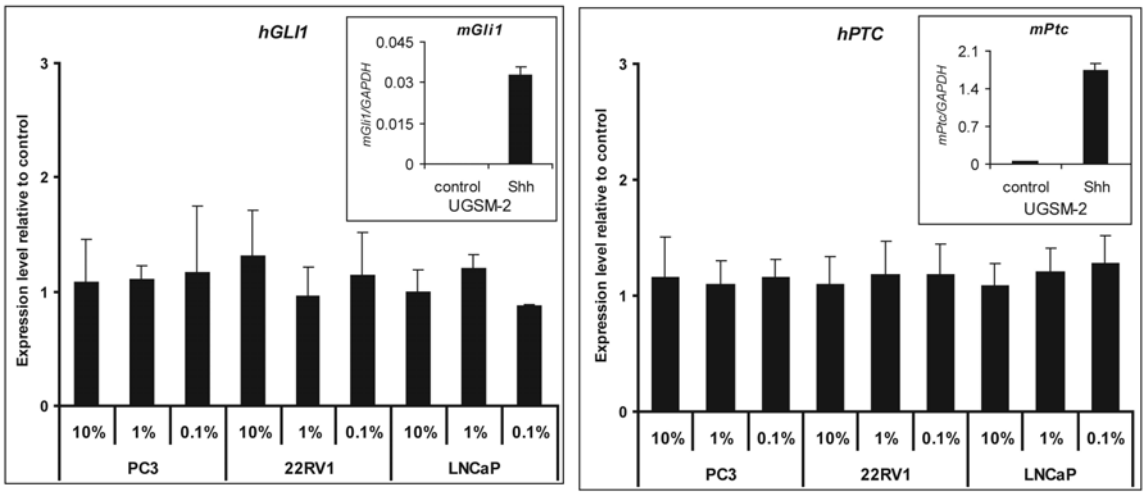

Figure 9. Treatment of Prostate cancer cell lines with 1 nM purified Shh peptide does not induce expression of Hh target genes Ptc and Gli1. (inset) Treatment of UGSM-2 mesenchymal cells with the same dose of Shh causes a ~100-fold increase in expression of Hh target genes Ptc and Gli1.

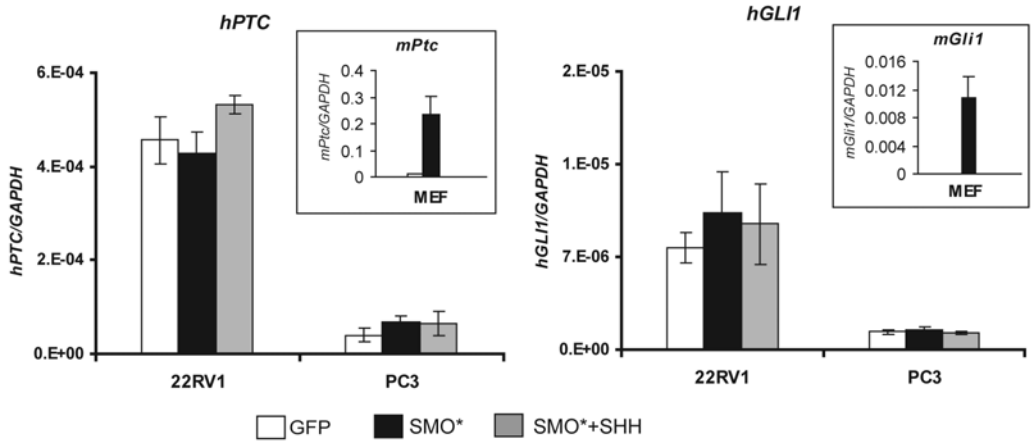

Figure 10. Expression of constitutively active Smo, an inducer of Hh signaling, fails to induce expression of Hh target genes in 22RV1 and PC-3 human prostate cancer cell lines, but the same expression construct faithfully induces Hh signaling in mouse embryonic fibroblasts (inset).

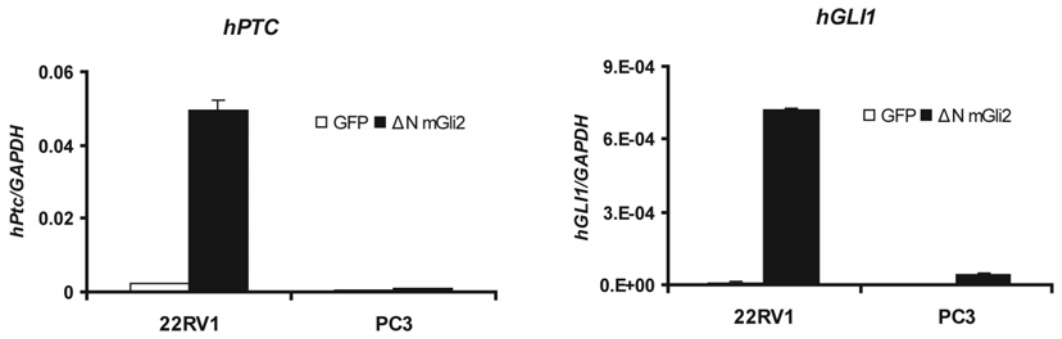

Figure 11. Expression of constitutively active Gli2 in 22RV1 or PC-3 cells induces Hh signaling.

Hh pathway activiy is lower in isolated epithelial cells than prostate tissue. In the study of human medulloblatomas, SaSai et al[4] reported shh pathway activity is down-regulated in cultured mouse tumor cells and those cells can not respond to Smo inhibitor any more even in vivo. Similar result has also been shown in the study of small-cell lung cancer[8]. Since prostate cancer cells can not respond to shh, we started to examine the Hh pathway activity in the isolated human epithelial cells and prostate cancer cells lines.

Comparison of Hh ligand expression in four prostate cancer cell lines showed that ligand expression was highest in PC3 and lowest in LNCaP (Figure 12a). Shh and Ihh expression in PC3 was of the same order of magnitude as in the fetal brain, but well below what is found in the normal adult prostate (Figure 12b). Four primary epithelial cell lines isolated from human benign prostate tissue as well as BPH1 immortalized prostate epithelial cells exhibited expression that is intermediate between LNCaP and PC3 (Figure 12c). Ptc and Gli1 are primary targets of Hh transcriptional activation. Ptc expression is highest in LNCaP and 22RV1, intermediate in PC3 and lowest in DU145 cells (Figure 13a). Gli1 expression was similar in all cell lines (Figure 13a). Ptc and Gli1 expression in these cell lines was generally comparable to expression in the four primary epithelial cell lines and BPH-1, but much lower than normal prostate tissue (Figure 13b). These studies reveal that the level of Hh ligand expression in all four cell lines is lower than that observed in pooled normal prostate specimens. Further, pathway activity in the four cell lines, as judged by Ptc and Gli1 expression, is also considerably lower than that observed in the pooled normal prostate specimens. Together these data do not suggest elevated Hh pathway activity in these cell lines.

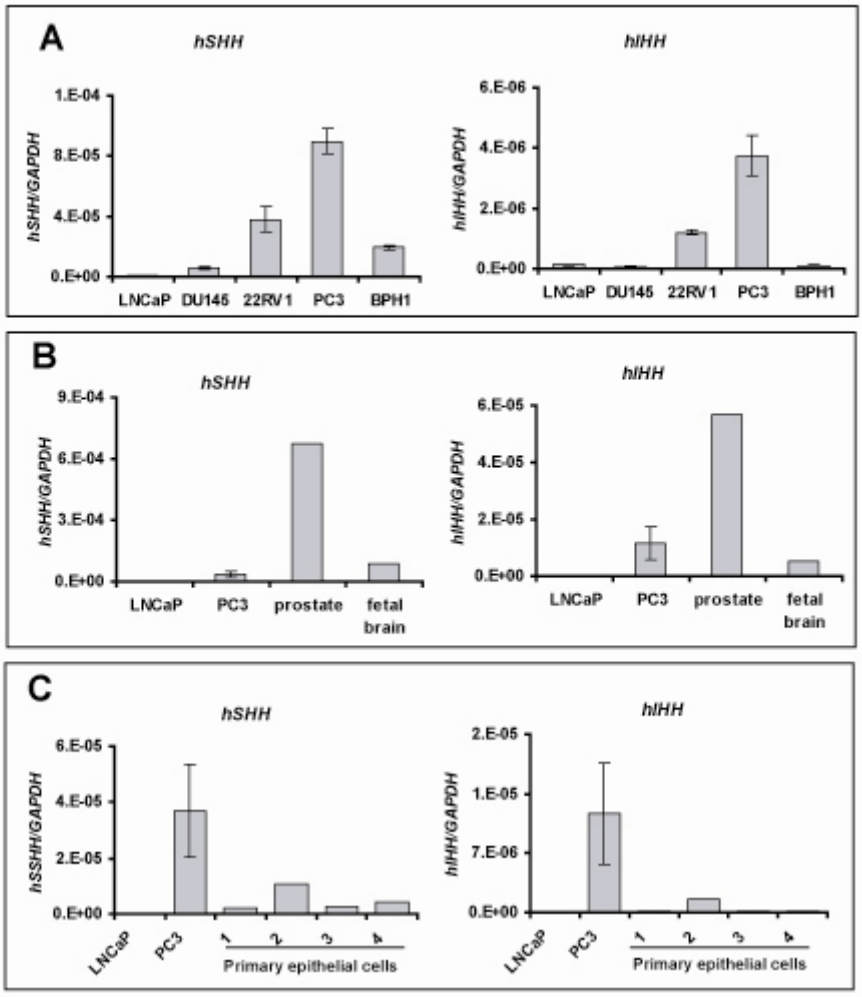

Figure 12 (A) Shh and Ihh expression in four prostate cancer cell lines (LNCaP, DU145, PC3 and 22RV1) and the immortalized BPH-1 cell line. (B) Comparison of expression in LNCaP and PC3 with expression in the human fetal brain and a pooled sample of normal adult prostate RNA. (C) Comparison of expression in LNCaP and PC3 with expression in four primary benign prostate epithelial cell lines.

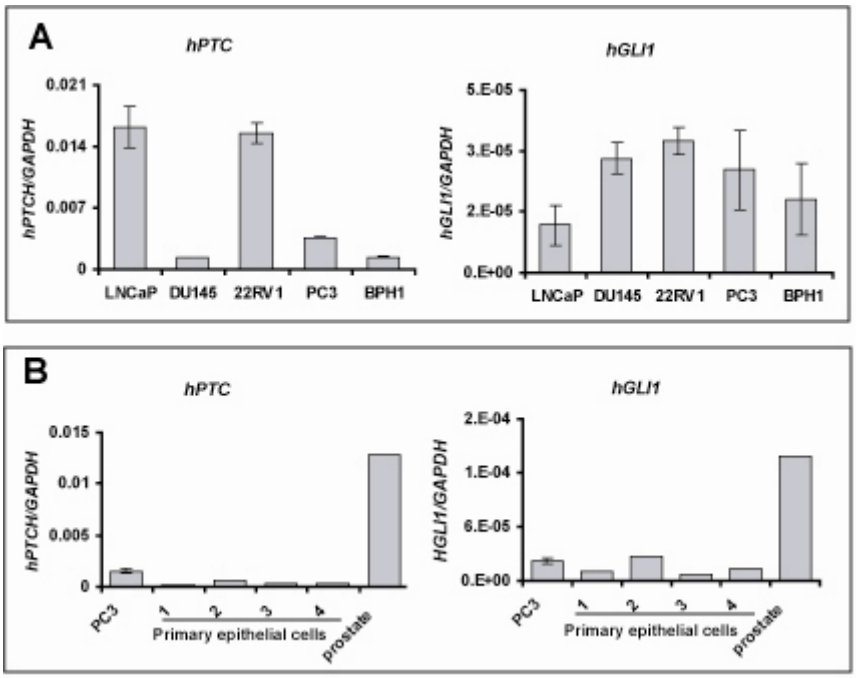

Figure 13 (A) Expression of the conserved Hh target genes Ptc and Gli1 in four prostate cancer cell lines (LNCaP, DU145, PC3 and 22RV1) and the immortalized BPH-1 cell line. (B) Comparison of Ptc and Gli1 expression in PC3 and four primary benign prostate epithelial cell li Figure 13 (A) Expression of the conserved Hh target genes Ptc and Gli1 in four prostate cancer cell lines (LNCaP, DU145, PC3 and 22RV1) and the immortalized BPH-1 cell line. (B) Comparison of Ptc and Gli1 expression in PC3 and four primary benign prostate epithelial cell lines.

Key research accomplishments:

We have generated and characterized Gli1 and Gli2 over-expression UGSM-2 cells.
We have developed prostate stromal cell lines lacking Gli1, Gli2, Gli3.

We have showed that Gli3 knock out cells increase tumor growth in the xenograft model.
We have showed that autocrine hedgehog signaling is not involved in growth of human prostate cancer cell lines.

Training experiences

I learned mammalian cell culture, transfection, retrovirus and andenovirus infection of mammalian cells.
I also learned how to do xenograft , tumor measurement, immunohistology.
In addition, I have learned to use flow cytometry to monitor cell proliferation, cell death and cells labeled by fluoresecent protein.

I have participated in numerous conferences including weekly lab meeting and journal club, monthly joint lab meeting with Dr. Richard E Peterson lab, prostate cancer group meeting and O' Brien center meeting. All these opportunity were provided by the sponsor (Wade Bushman, M.D., Ph.D.).

Reportable outcomes:

UGSM-2 cell lines over-expressing Gli1 or Gli2.

Gli1, Gli2, Gli3 knock out UGSM cell lines.

A manuscript has been published in the Experimental Cell Research. R.J.Lipinski, J.Gipp, J.Zhang, J.D.Doles and W.Bushman: Unique and complimentary activities of the Gli transcription factors in Hedgehog signaling(Experimental cell Research, 312:1925-1938,2006).

J, Zhang, R.J.Lipinski, A, Shaw, and W. Bushman : Autocrine hedgehog signaling is not involved in growth of human prostate cancer cells in vitro. Journal of Urology, In Press.

Conclusions:

I have generated prostate stromal cell lines over-expressing Gli1 or Gli2. $Gli1^{(-/-)}$, $Gli2^{(-/-)}$ and $Gli3^{(-/-)}$ knockout UGSM cells were also isolated. Co-injecting UGSM-2 cells over-expressing Gli1 with LNCaP cells did not accelerate tumor growth. Real time PCR result showed that mGli1 was not activated in the tumor compared to control, suggesting either loss of expression or diluted loss of over-expression cells. Over-expression of Gli2

resulted in sarcoma formation making assessment of its role in tumor growth unreliable. UGSM-2 cells Gli3 knock out cells activate the Shh pathway, and are sufficient to promote tumor growth in the LNCaP xenograft model. Shh pathway activity is down-regulated in cultured prostate epithelial cells, and commonly used prostate cancer cells are not capable of Hh signal transduction. All these result suggest that the growth effects of LNCaP over-expressing shh on xenograft tumors are mediated by paracrine interactions with other cells in the tumor.

I have successfully completed the specific aims, as outlined above, which has provided me with excellent training in prostate cancer research.

References:

1. Fan, L., Pepicelli, C. V., Dibble, C. C., Catbagan, W., Zarycki, J. L., Laciak, R. et al.: Hedgehog signaling promotes prostate xenograft tumor growth. Endocrinology, **145:** 3961, 2004

2. Karhadkar, S. S., Bova, G. S., Abdallah, N., Dhara, S., Gardner, D., Maitra, A. et al.: Hedgehog signalling in prostate regeneration, neoplasia and metastasis. Nature, **431:** 707, 2004

3. Sanchez, P., Hernandez, A. M., Stecca, B., Kahler, A. J., DeGueme, A. M., Barrett, A. et al.: Inhibition of prostate cancer proliferation by interference with SONIC HEDGEHOG-GLI1 signaling. Proc Natl Acad Sci U S A, **101:** 12561, 2004

4. Sasai, K., Romer, J. T., Lee, Y., Finkelstein, D., Fuller, C., McKinnon, P. J. et al.: Shh pathway activity is down-regulated in cultured medulloblastoma cells: implications for preclinical studies. Cancer Res, **66:** 4215, 2006

5. shaw, A., Bushman, W.: Hedgehog singnaling in the prostate. journal of Urology, **In press.**

6. Shaw, A., Papadopoulos, J., Johnson, C., Bushman, W.: Isolation and characterization of an immortalized mouse urogenital sinus mesenchyme cell line. Prostate, **66:** 1347, 2006

7. Sheng, T., Li, C., Zhang, X., Chi, S., He, N., Chen, K. et al.: Activation of the hedgehog pathway in advanced prostate cancer. Mol Cancer, **3:** 29, 2004

8. Vestergaard, J., Pedersen, M. W., Pedersen, N., Ensinger, C., Tumer, Z., Tommerup, N. et al.: Hedgehog signaling in small-cell lung cancer: frequent in vivo but a rare event in vitro. Lung Cancer, **52:** 281, 2006

Appendix:

Two manuscripts attached

LACK OF DEMONSTRABLE AUTOCRINE HEDGEHOG SIGNALING IN HUMAN PROSTATE CANCER CELL LINES

JINGXIAN ZHANG, ROBERT LIPINSKI, AUBIE SHAW, JERRY GIPP AND WADE BUSHMAN

From the Department of Surgery and the McArdle Laboratory for Cancer Research, University of Wisconsin, Madison, Wisconsin

Please send correspondence to: Department of Surgery, University of Wisconsin, 600 Highland Avenue, Madison, WI 53792 (telephone: 608-265-8705, FAX: 608-265-8133, e-mail: bushman@surgery.wisc.edu).

This work was supported by the Department of Defense Prostate Cancer Research Program grants W81XWH-04-1-0263 and W81XWH-04-1-0157.

Running title: Lack of autocrine Hh signaling in prostate cancer cell lines

Key words: hedgehog pathway, prostate cancer, cell lines, cyclopamine

Abbreviations: Hedgehog; Hh, Patched; Ptc, Sonic Hedgehog; Shh, Indian Hedgehog; Ihh, Smoothened; Smo, Hedgehog-Interacting Protein ; Hip, Suppressor of Fused; SuFu, m; mouse gene, h; human gene

Word count: 3169

ABSTRACT
Introduction: Several recent reports have highlighted the role of Hedgehog (Hh) signaling in prostate cancer. However, the relative contributions of autocrine and paracrine Hh signaling to tumor growth and progression is unclear and efforts to model autocrine signaling for drug development have been hampered by conflicting reports of the presence or absence of autocrine signaling in established human prostate cancer cell lines.
Materials and Methods: We comprehensively characterized the expression of Hh pathway genes in three prostate cancer cell lines (LNCaP, PC3 and 22RV1) and examined their response to Shh ligand and to the Hh pathway inhibitor cyclopamine.
Results: Expression of Hh ligand, Ptc and Gli1 in all three cell lines is lower than the level of expression in normal human prostate tissue. All three cell lines exhibited Hh target gene activation when transfected with an activated form of Gli2, but none showed a detectable transcriptional response to Hh ligand or to transfection with an activated form of Smo. Further, treatment with the Hh pathway inhibitor cyclopamine did not inhibit Hh target gene expression in any of the three prostate cancer cell lines even though cyclopamine did inhibit proliferation in culture.
Conclusions: LNCaP, PC3 and 22RV1 show no evidence of autocrine signaling by ligand dependent mechanisms, and cyclopamine-mediated inhibition of growth in culture occurs without of any discernable effect on canonical Hh pathway activity.

INTRODUCTION

Hedgehog (Hh) signaling is required for normal prostate development[1-7]. The Hh ligands Shh and Ihh are expressed in the epithelium of the urogenital sinus and the tips of the developing ducts. Expression of the Hh target genes Ptc and Gli1 primarily in the adjacent mesenchyme reflects a major component of paracrine signaling from the epithelium to the mesenchyme, but focal expression of Ptc and Gli1 in the epithelium at the tips of the growing ducts has been interpreted as evidence of localized autocrine signaling[6, 8].

Several studies have shown active Hh signaling in human prostate cancer and provided evidence that Hh signaling accelerates tumor growth[9-12]. Xenograft studies have shown that paracrine Hh signaling alone can accelerate tumor growth, however, other studies suggest that autocrine signaling may also play a central role. Some studies suggest the operation of ligand-dependent autocrine signaling while others suggest the operation of ligand-independent mechanisms of pathway activation resulting from mutation. The development of pharmacologic inhibitors of Hh signaling for use in treating prostate cancer depends upon further studies to define the relative contribution of autocrine and paracrine signaling in human prostate cancer and development of in vitro models for drug development and testing. Divergent reports on the presence or absence of autocrine signaling in several prostate cancer cell lines have slowed research and development. We report here a comprehensive, mechanistic study of autocrine signaling in commonly used prostate cancer cell lines.

MATERIALS AND METHODS

Cell Lines. Prostate cancer cell lines were purchased from American Type Culture Collection (ATCC, Manassas, VA) and maintained in the recommended medium. BPH1 cells were a generous gift from Simon Hayward (Vanderbilt University, Nashville, TN) and were grown in RPMI 1640 medium with 5% fetal calf serum (FCS). UGSM-2 cells[13] and MEFs were isolated

in our laboratory. Four cDNA samples from independent human prostate epithelial cultures were kindly provided by David Jarrard (University of Wisconsin, Madison, WI). Human prostate total RNA and fetal brain total RNA were purchased from BD Biosciences (Palo Alto, CA). Human prostate total RNA was pooled from normal prostates of 32 Caucasian males ages 21-50. Human fetal brain total RNA is from normal fetal brains pooled from 21 spontaneously aborted male/female Caucasian fetuses, ages 26-40 weeks. Cells were plated in a 24-well plate at 1×10^5 cells/well. To assay gene expression after Shh/cyclopamine treatment, serum concentration was reduced to 1% after 1 day attachment, and either 1nM, 10nM octylated N-Shh (Curis, Inc., Cambridge, MA) or 5μM cyclopamine (Toronto Research Chemicals, Ontario, Canada) was added to the medium and RNA was harvested after 48 hours. A 1nM concentration of octylated N-Shh equates with a 400nM dose of unmodified N-Shh.

Co-culture. UGSM-2 cells were plated at 1.6×10^5 cells/well in a 12 well plate. After 24 hours, cancer cells were added on top of UGSM-2 cells at the same density. 5μM cyclopamine or 1nM octylated N-Shh was added to the medium and RNA was harvested after 24 hours.

Gli-luciferase assay. Shh LIGHTII cells expressing Gli-responsive Firefly luciferase and TK-Renilla were generously provided by Dr. Philip Beachy. Cells were plated in 10% FBS at 90% confluence in Primaria multiwell plates and attached overnight. Media was replaced with 1% FBS +/- Shh peptide at given concentrations. After 48 hrs, Firefly and Renilla luciferase activity was assayed using the Dual Luciferase Assay System (Promega).

Cell proliferation assay. Cells were set in a 24-well plate at a density of 20,000 cells/well and allowed to attach overnight. The concentration of FCS in the media was changed to 2%, and various concentrations of cyclopamine were added. Cells were grown for 4 days, harvested for RNA or trypsinized and counted by Vi-cell XR cell viability analyzer (Beckman Coulter, Fullerton, CA).

Adenovirus infection. Adenovirus constructs carrying ΔNmGli2-GFP, hSmo*-GFP or GFP alone[14] were kindly provided by Chen-Ming Fan (Carnegie Inst, Baltimore, MD). Cells were plated in a 24-well plate at 1×10^5 cells/well. After 24 hours attachment, media was replaced with 1% FCS +/- adenovirus at a multiplicity of infection of 25-100 PFU/cell +/- Shh peptide. Under these conditions, >90% of cells were infected according to GFP fluorescence analysis by flow cytometry.

RNA isolation and real time RT-PCR. RNA was isolated using Qiagen (Valencia, CA) RNeasy RNA isolation Kits and subjected to on-column DNase digestion. cDNA was generated following standard protocols. Gene expression was assayed by real time RT-PCR on BioRad iCycler instrument (Hercules, CA) using glyceraldehyde-3-phosphate dehydrogenase (GAPDH) as an internal standard gene. Primer sequences used in this experiment are listed in Table I.

Statistical analysis. Each experiment was repeated 3 times independently. An unpaired *t*-test was used to determine if statistically significant differences exist between treatment groups.

RESULTS

Hh pathway activity in prostate cancer cell lines. Comparison of Hh ligand expression in four prostate cancer cell lines showed that ligand expression was highest in PC3 and lowest in LNCaP (Figure 1a). Shh and Ihh expression in PC3 was of the same order of magnitude as in the fetal brain, but well below what is found in the normal adult prostate (Figure 1b). Four primary epithelial cell lines isolated from human benign prostate tissue as well as BPH1 immortalized prostate epithelial cells exhibited expression that is intermediate between LNCaP and PC3 (Figure 1c). Ptc and Gli1 are primary targets of Hh transcriptional activation. Ptc expression is highest in LNCaP and 22RV1, intermediate in PC3 and lowest in DU145 cells (Figure 2a). Gli1 expression was similar in all cell lines (Figure 2a). Ptc and Gli1 expression in these cell lines was generally comparable to expression in the four primary epithelial cell lines and BPH-1, but much lower than normal prostate tissue (Figure 2b). These studies reveal that the level of Hh ligand expression in all four cell lines is lower than that observed in pooled normal prostate specimens. Further, pathway activity in the four cell lines, as judged by Ptc and Gli1 expression, is also considerably lower than that observed in the pooled normal prostate specimens. Together these data do not suggest elevated Hh pathway activity in these cell lines.

We noted that Ptc and Gli1 expression in the cell lines does not track the level of endogenous Hh ligand expression, suggesting that target gene expression may not be linked to ligand-dependent pathway activation. We therefore examined responsiveness of the tumor cell lines to exogenous Hh ligand. Using 1nM and 10nM concentrations of octylated Shh peptide which elicit 75% and 100% of maximal induction of Gli-luciferase reporter activity in NIH 3T3 cells, respectively (Figure 3a), we observed no detectable increase in the expression of either Ptc or Gli1 in any of the tumor cell lines tested (Figure 3b and not shown). Since serum levels are known to affect Hh responsiveness in vitro (unpublished observation), we treated cells with 1nM Shh under a range of serum conditions. 1nM Shh was unable to induce expression of either Ptc or Gli1 under 10%, 1% or 0.1% FCS conditions (Figure 3c). To verify activity of Shh in the same assays, we treated a urogenital sinus mesenchyme cell line, UGSM2, in medium containing 1% FCS with 1nM Shh (Figure 3b, 3c insert). These observations are consistent with our previous observation that LNCaP stably overexpressing Shh (LN-Shh) exhibited no evidence of pathway activation[9].

Intracellular Hh signaling in PCa cell lines. Each prostate cancer cell line expresses mRNA for the major components of the Hh signal transduction pathway (Figure 4a) although the relative abundance of each factor shows considerable variation (Figure 4b). Lack of responsiveness to Shh ligand could result from 3 different mechanisms: a block in ligand binding and transmembrane signal transduction, a defect in the intracellular signal transduction mechanism or a specific block in the transcription of Ptc and Gli1 in response to Hh pathway activation. To distinguish between these, we transiently expressed activated forms of Smo and Gli2 that have been shown to activate expression of Hh target genes in many cell types[9, 15, 16]. The activated form of hSmo (Smo*) activates the intracellular signal transduction pathway and indirectly activates target gene transcription, whereas, the activated form of mGli2 (ΔNmGli2) is considered a direct transcriptional activator of Hh target genes. Expression of Smo* in PC3 and 22RV1 cells did not induce expression of Ptc and Gli1 in either cell line, whereas it induced robust Ptc and Gli1 expression in both mouse embryonic fibroblasts (MEFs) and UGSM-2 cells (Figure 5a insert and not shown). In contrast, expression of ΔNmGli2 induced Hh target gene expression in both cell lines. It induced robust expression of both Ptc and Gli1in 22RV1, and induced robust expression of Gli1 but not Ptc in PC3 (Figure 5b). The simplest explanation for

the increase in Gli1 but not Ptc expression in PC3 cells is that Gli1 is a more sensitive marker of induction because of its lower basal level of expression. These studies suggest that the failure of PC3 and 22RV1 to respond to Hh ligand with induction of Ptc and Gli1 results from a defect in the intracellular signal transduction mechanism in these cell lines.

Effect of cyclopamine on Hh signaling. The plant steroidal alkaloid cyclopamine inhibits Hh signaling by preventing activation of Smo[17]. To examine endogenous, Smo-dependent Hh signaling in the cancer cells, we examined the ability of 5 μM cyclopamine to block transcription of Hh target genes Ptc and Gli1 in the cell lines. Regardless of whether the assay was performed in 10%, 1% or 0.1% FCS, we observed no significant effect on Ptc or Gli1 expression in any prostate cancer cell line (Figure 6). We also observed no effect of cyclopamine when the assay was performed in the presence of 1nM exogenous Shh peptide (data not shown). In contrast, 5 μM cyclopamine completely blocked Hh pathway activity in UGSM-2 cells stimulated with 1 nM Shh (Figure 6 insert). These findings, which demonstrate a lack of effect of the Smo antagonist cyclopamine, complement the lack of target gene activation by transfection with Smo* and further suggest the absence of Smo-dependent autocrine signaling.

Effect of cyclopamine on tumor cell proliferation. Hh pathway activity has been implicated as a stimulus of prostate cancer cell proliferation, and inhibition of tumor cell proliferation in vitro by cyclopamine has been attributed to specific inhibition of the Hh pathway [10-12]. We examined the effect of cyclopamine on growth of cancer cell lines in culture and correlated effects on proliferation with expression of the Hh target genes Ptc and Gli1. Treatment with 5 μM cyclopamine resulted in a decreased number of LNCaP cells after four days in culture, a slight decrease in the number of 22RV1 cells and no change in the number of PC3 cells (Figure 7). Treatment with 10 μM cyclopamine significantly reduced the number of cells after four days in all three tumor cell lines, but this effect did not correlate with a significant inhibition of Hh pathway activity as measured by Ptc and Gli1 expression (Figure 7 insert). These observations suggest that the inhibition of tumor cell proliferation in vitro by cyclopamine does not result from a specific effect on Hh pathway activity.

Cyclopamine has been reported to inhibit growth of PC3 tumor xenografts[10]. This has been attributed to chemical inhibition of autocrine signaling in the xenograft, however, our studies do not demonstrate significant autocrine signaling in this cell line. To examine the possibility that cyclopamine might interfere with tumor growth by inhibiting Hh pathway activity in the tumor stroma, we examined the effect of cyclopamine on PC3 tumor cells grown in co-culture with UGSM-2 stromal cells. LNCaP cells over-expressing Shh[9] were similarly co-cultured with UGSM-2 cells as a positive control for robust paracrine Hh pathway activation. Expression of the conserved Hh target genes Ptc and Gli1 was measured in human cancer cells and mouse stromal cells by real time RT-PCR using species-specific primers. Cyclopamine had no effect on hPtc and hGli1 transcription in the cancer cells themselves (Figure 8 top). In contrast, cyclopamine dramatically reduced mPtc and mGli1 transcription in UGSM-2 cells co-cultured with either PC3 or LN-Shh cells (Figure 8 bottom).

DISCUSSION

Our previous studies of Hh signaling in normal and neoplastic human prostate demonstrated comparable levels of expression of Hh ligand and Gli1 in specimens of benign and localized

prostate cancer, with a suggestion of higher level expression in locally advanced and/or androgen independent prostate cancer. We demonstrated expression of Shh in the tumor epithelium with localization of Gli1 predominantly in the peri-glandular tumor stroma, and used the LNCaP xenograft to show that paracrine Shh signaling accelerates tumor growth[11]. Recently, we have shown that the paracrine effect of Shh signaling on tumor growth can be influenced by the composition of the tumor stroma (unpublished observations) and we therefore speculate that Hh signaling may exert different growth effects in the normal prostate and in prostate cancer depending on the composition and/or reactivity of the stromal compartment. Several other studies examining the expression of Shh in localized and metastatic prostate cancer suggested that increased Shh expression in localized tumors exerts a combination of autocrine and paracrine signaling activity, and dramatically increases pathway activity in metastatic disease[10-12]. The possible contribution of autocrine signaling to tumor growth was examined by studying the effect of cyclopamine, anti-Shh antibody and Gli1 transfection on the proliferation of several human prostate cancer cell lines including LNCaP, PC3 and 22RV1[10-12](Also see Shaw and Bushman, this issue, for review). The studies suggested that these cell lines were characterized by high levels of Hh pathway activity, that cyclopamine could inhibit tumor cell proliferation in culture by a Hh specific mechanism and that cyclopamine could exert a dose dependent inhibition of xenograft tumor growth. These studies clearly suggested that autocrine pathway activity promotes tumor cell proliferation and treatment with Hh inhibitors might be a promising avenue for treatment. However, the results reported in these papers are not entirely consistent. For example, Karhadkar et al[10] found that anti-Shh blocking antibody inhibited PC3 proliferation, whereas Sanchez et al[11] found that PC3 proliferation was unaffected by either anti-Shh blocking antibody or exogenous Shh. Moreover, they conflicted with our previous studies showing an absence of Hh pathway responsiveness in LNCaP[9]. For this reason, we undertook a comprehensive analysis of autocrine Hh pathway signaling in these cell lines.

Our studies show that LNCaP, DU145, PC3 and 22RV1 all express Hh ligands and other components of Hh signal transduction. The level of ligand expression varies, with the highest level of mRNA expression present in PC3 and being comparable to the robust level of expression observed in the fetal brain. Even so, this is below the level of expression in a pooled normal prostate sample composed of 32 prostate specimens from men 21-50 years of age. The fact that expression is lower in all prostate cancer cell lines examined and in four primary prostate epithelial cell lines than in the normal prostate is intriguing and might suggest that in vitro culture conditions reduce Hh ligand expression. Similarly, the expression of Ptc and Gli1 in these cell lines is much lower than in the normal prostate and might reflect a loss of autocrine signaling in vitro or signify that the primary domain of Ptc and Gli1 expression in the intact prostate is in the glandular stroma.

Since the tumor cell lines express the Hh ligands Shh and Ihh, pathway activity could result from ligand-dependent autocrine pathway activation. However, our studies of LNCaP, PC3 and 22RV1 found no evidence for a transcriptional response to exogenous Hh ligand. While the lack of response of LNCaP was consistent with our previous studies [11], the unresponsiveness of PC3 and 22RV1 was unexpected and contradictory to previously reported studies. To validate these observations, we examined the effect of intracellular pathway activation in PC3 and 22RV1 cells. Infection with an adenoviral vector expressing activated Smo did not induce Ptc or Gli1 transcription in either cell line. This observation argues that the canonical Smo-mediated signal

transduction pathway is non-functional. This was confirmed by showing that transcriptional activation of Hh target genes Ptc and Gli1 could be achieved in these cells by infection with an adenoviral vector expressing an activated form of Gli2 (ΔNmGli2). These studies, which demonstrate a non-functional post-receptor signal transduction pathway in both PC3 and LNCaP, are consistent with a lack of responsiveness to Hh ligand.

Cyclopamine inhibits Hh signaling by binding to and preventing the activation by Smo[17]. We observed no changes in the expression of Hh target genes Ptc and Gli1 in LNCaP, PC3 or 22RV1 treated with 5 μM cyclopamine under a range of culture conditions, a finding consistent with our transfection studies demonstrating a failure to induce Smo-mediated Hh pathway activation. These observations stand in contrast to the studies of Karhadkar et al[10]. However, those authors examined the effect of cyclopamine on expression of a Gli-reporter construct, rather than expression of endogenous Ptc and Gli1. It is possible that they observed an effect of cyclopamine on reporter gene expression that does not accurately reflect the effect of cyclopamine on the expression of endogenous target genes.

We observed that treatment of cells in culture with 10 μM cyclopamine decreased cell number without any discernable effect on Hh pathway activity. These findings strongly suggest that inhibition of cell proliferation is not the result of canonical Smo-mediated Hh pathway inhibition but rather a non-specific or toxic effect. But, how can we reconcile these observations with previously published studies showing a dramatic effect of cyclopamine on PC3 and 22RV1 xenograft tumors? One explanation is that PC3 and 22RV1 cells growing in vivo exhibit a different phenotype and are susceptible to cyclopamine-mediated inhibition of canonical pathway activity. Another is that the effect of cyclopamine on xenograft tumor growth is mediated through an effect on stromal cells responding to Hh ligand produced by the tumor cells. This putative mechanism is supported by our co-culture studies and suggests that the effect of Hh inhibitors on tumor growth may include effects on paracrine as well as autocrine pathway activity.

Efforts are currently underway to develop Hh pathway inhibitors for clinical use. A critical step in this process is the development and use of appropriate cell lines and/or tumor models that are dependent on Hh signaling for growth. It has been assumed, based on previously published studies, that human prostate cancer and commonly used prostate cancer cell lines both exhibit robust autocrine signaling. However, the experiments reported here reveal no evidence for autocrine Hh signaling in the most commonly used human prostate cancer cell lines under standard culture conditions and found no evidence that the Hh inhibitor cyclopamine could inhibit cell proliferation by a specific effect on Hh pathway activity. These findings caution against using these cell lines as an in vitro model of autocrine Hh signaling in prostate cancer. It is possible that the xenografts made with PC3 and 22RV1 might exhibit autocrine signaling that cannot be modeled in cell culture, but it is also likely that xenografts made with these Hh-expressing cell lines also involve paracrine signaling interactions. Therefore, investigators testing the effect of Hh pathway inhibitors on prostate tumor xenografts should evaluate the effects of these agents on paracrine signaling as well as autocrine pathway activity.

REFERENCES

1. Podlasek, C. A., Barnett, D. H., Clemens, J. Q., Bak, P. M., Bushman, W.: Prostate development requires Sonic hedgehog expressed by the urogenital sinus epithelium. Dev Biol, **209:** 28, 1999

2. Lamm, M. L., Catbagan, W. S., Laciak, R. J., Barnett, D. H., Hebner, C. M., Gaffield, W. et al.: Sonic hedgehog activates mesenchymal Gli1 expression during prostate ductal bud formation. Dev Biol, **249:** 349, 2002

3. Wang, B. E., Shou, J., Ross, S., Koeppen, H., De Sauvage, F. J., Gao, W. Q.: Inhibition of epithelial ductal branching in the prostate by sonic hedgehog is indirectly mediated by stromal cells. J Biol Chem, **278:** 18506, 2003

4. Freestone, S. H., Marker, P., Grace, O. C., Tomlinson, D. C., Cunha, G. R., Harnden, P. et al.: Sonic hedgehog regulates prostatic growth and epithelial differentiation. Dev Biol, **264:** 352, 2003

5. Berman, D. M., Desai, N., Wang, X., Karhadkar, S. S., Reynon, M., Abate-Shen, C. et al.: Roles for Hedgehog signaling in androgen production and prostate ductal morphogenesis. Dev Biol, **267:** 387, 2004

6. Pu, Y., Huang, L., Prins, G. S.: Sonic hedgehog-patched Gli signaling in the developing rat prostate gland: lobe-specific suppression by neonatal estrogens reduces ductal growth and branching. Dev Biol, **273:** 257, 2004

7. Doles, J., Shi, X., Bushman, W.: Functional Redundancy of Hedgehog Signaling Regulating Mouse Prostate Development. Dev. Biol, **in press**, 2005

8. Gao, N., Ishii, K., Mirosevich, J., Kuwajima, S., Oppenheimer, S. R., Roberts, R. L. et al.: Forkhead box A1 regulates prostate ductal morphogenesis and promotes epithelial cell maturation. Development, **132:** 3431, 2005

9. Fan, L., Pepicelli, C. V., Dibble, C. C., Catbagan, W., Zarycki, J. L., Laciak, R. et al.: Hedgehog signaling promotes prostate xenograft tumor growth. Endocrinology, **145:** 3961, 2004

10. Karhadkar, S. S., Bova, G. S., Abdallah, N., Dhara, S., Gardner, D., Maitra, A. et al.: Hedgehog signalling in prostate regeneration, neoplasia and metastasis. Nature, **431:** 707, 2004

11. Sanchez, P., Hernandez, A. M., Stecca, B., Kahler, A. J., DeGueme, A. M., Barrett, A. et al.: Inhibition of prostate cancer proliferation by interference with SONIC HEDGEHOG-GLI1 signaling. Proc Natl Acad Sci U S A, **101:** 12561, 2004

12. Sheng, T., Li, C., Zhang, X., Chi, S., He, N., Chen, K. et al.: Activation of the hedgehog pathway in advanced prostate cancer. Mol Cancer, **3:** 29, 2004

13. Shaw, A., Papadopoulos, J., Johnson, C., Bushman, W.: Isolation and Characterization of an Immortalized Mouse Urogenital Sinus Mesenchyme Cell Line. The Prostate, **in press**, 2005

14. Buttitta, L., Mo, R., Hui, C. C., Fan, C. M.: Interplays of Gli2 and Gli3 and their requirement in mediating Shh-dependent sclerotome induction. Development, **130:** 6233, 2003

15. Taipale, J., Chen, J. K., Cooper, M. K., Wang, B., Mann, R. K., Milenkovic, L. et al.: Effects of oncogenic mutations in Smoothened and Patched can be reversed by cyclopamine. Nature, **406:** 1005, 2000

16. Xie, J., Murone, M., Luoh, S. M., Ryan, A., Gu, Q., Zhang, C. et al.: Activating Smoothened mutations in sporadic basal-cell carcinoma. Nature, **391:** 90, 1998

17. Chen, J. K., Taipale, J., Cooper, M. K., Beachy, P. A.: Inhibition of Hedgehog signaling by direct binding of cyclopamine to Smoothened. Genes Dev, **16:** 2743, 2002

Table I. Sequences of quantitive real time RT-PCR Primers

Gene	Forward Primer	Reverse Primer
mGAPDH	AGCCTCGTCCCGTAGACAAAAT	CCGTGAGTGGAGTCATACTGGA
mPatched	CTCTGGAGCAGATTTCCAAGG	TGCCGCAGTTCTTTTGAATG
mGli1	GGAAGTCCTATTCACGCCTTGA	CAACCTTCTTGCTCACACATGTAAG
hGAPDH	CCACATCGCTCAGACACCAT	GCAACAATATCCACTTACCAGAGTTAA
hPTCH	CGCTGGGACTGCTCCAAGT	GAGTTGTTGCAGCGTTAAAGGAA
hGLI1	AATGCTGCCATGGATGCTAGA	GAGTATCAGTAGGTGGGAAGTCCATAT
hGLI2	AGCCAGGAGGGCTACCAC	CTAGGCCAAAGCCTGCTGTA
hGLI3	ATCATTCAGAACCTTTCCCATAGC	TAGGGAGGTCAGCAAAGAACTCAT
hSHH	AAGGACAAGTTGAACGCTTTGG	TCGGTCACCCGCAGTTTC
hIHH	CACCCCCAATTACAATCCAG	AGATAGCCAGCGAGTTCAGG
hSmoothened	ACCTATGCCTGGCACACTTC	GTGAGGACAAAGGGGAGTGA
hHIP	CATGTCGTCATGGAGGTGTC	TCACTCTGCGGATGTTTCTG
hFused	GAGGGTGTACAAGGGTCGAA	TGCAAATTCCTCAGCTCCTT
hSufu	CGGAGGGGAGAGACCATATT	CACTTGGCACTGACACCACT

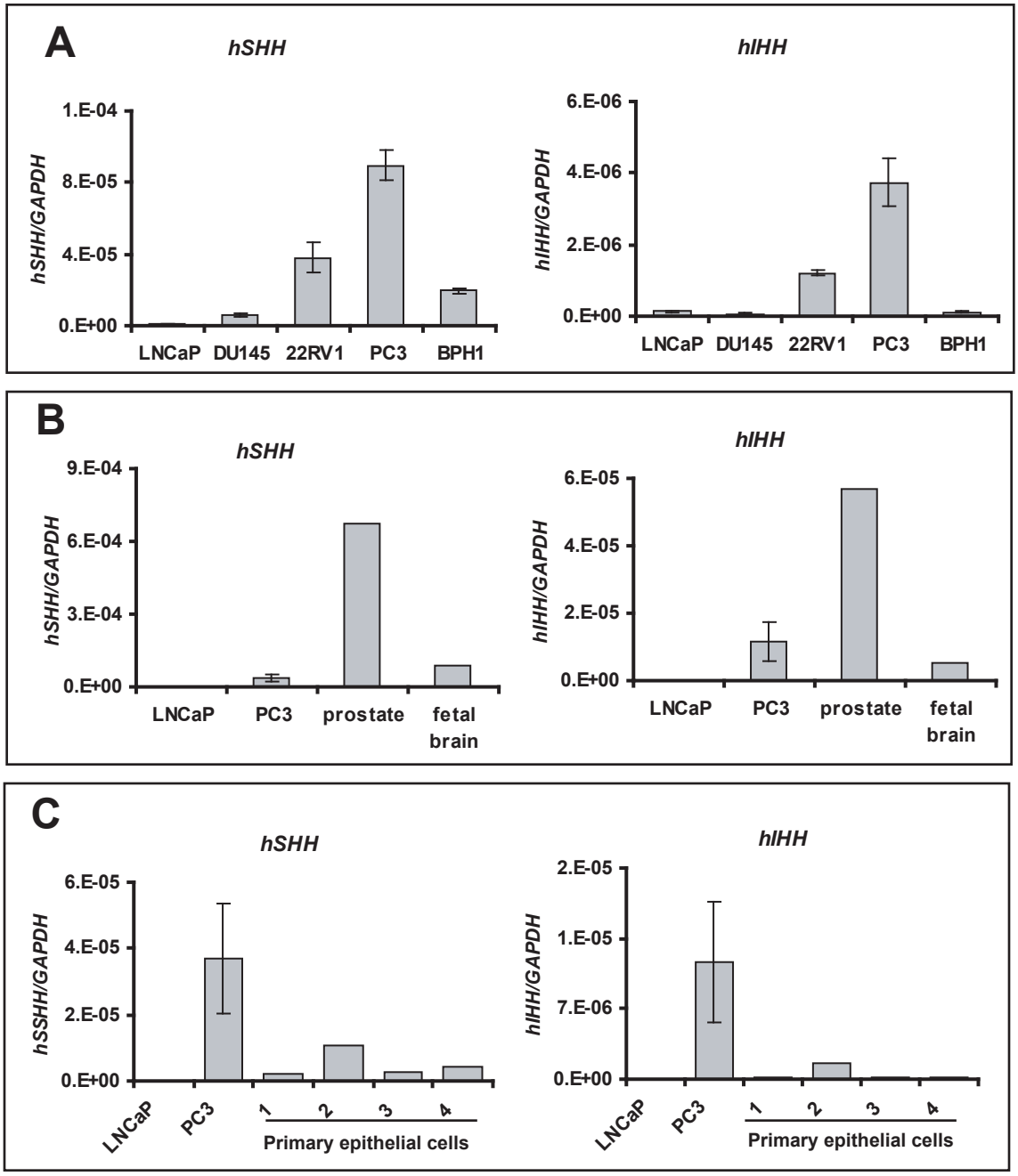

Figure 1 (A) Shh and Ihh expression in four prostate cancer cell lines (LNCaP, DU145, PC3 and 22RV1) and the normal human BPH-1 cell line. (B) Comparison of expression in LNCaP and PC3 with expression in the human fetal brain and a pooled sample of normal adult prostate RNA. (C) Comparison of expression in LNCaP and PC3 with expression in four primary benign prostate epithelial cell lines.

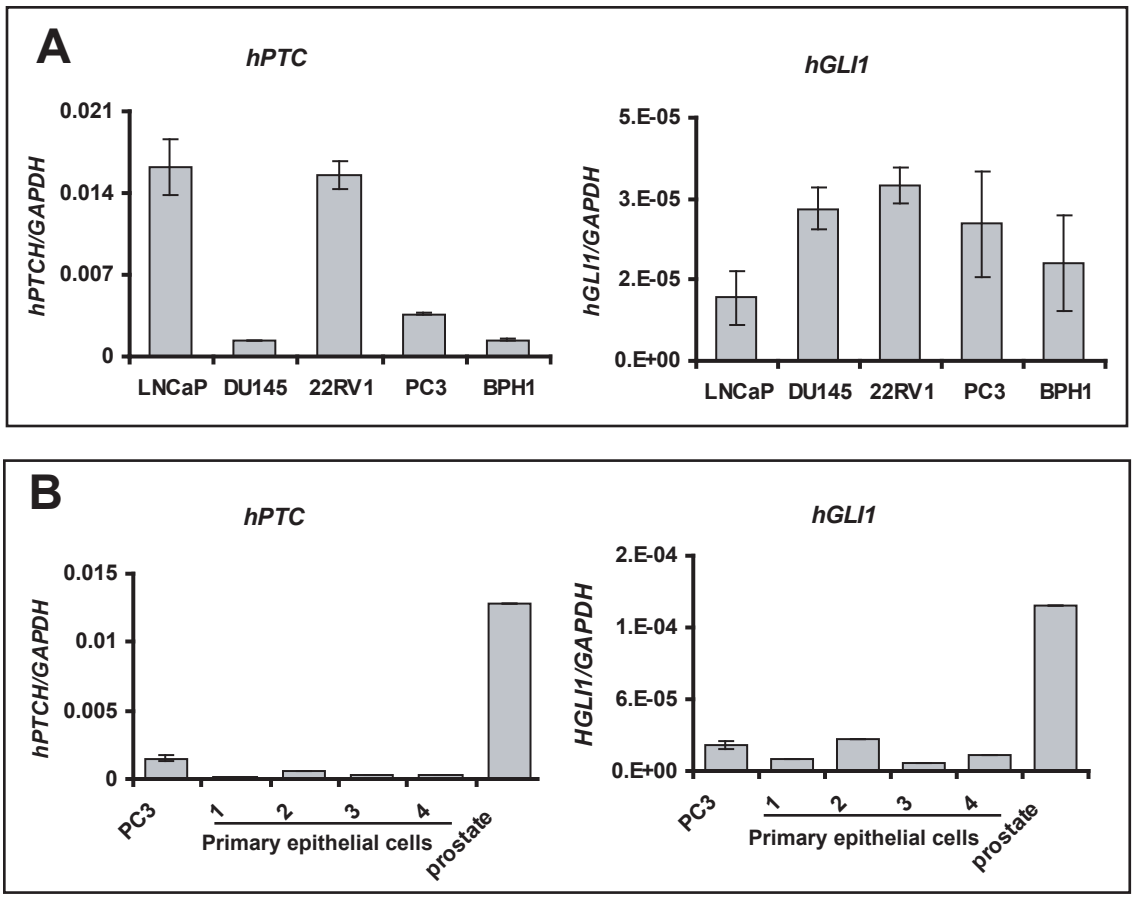

Figure 2 (A) Expression of the conserved Hh target genes Ptc and Gli1 in four prostate cancer cell lines (LNCaP, DU145, PC3 and 22RV1) and the normal human BPH-1 cell line. (B) Comparison of Ptc and Gli1 expression in PC3 and four primary benign prostate epithelial cell lines.

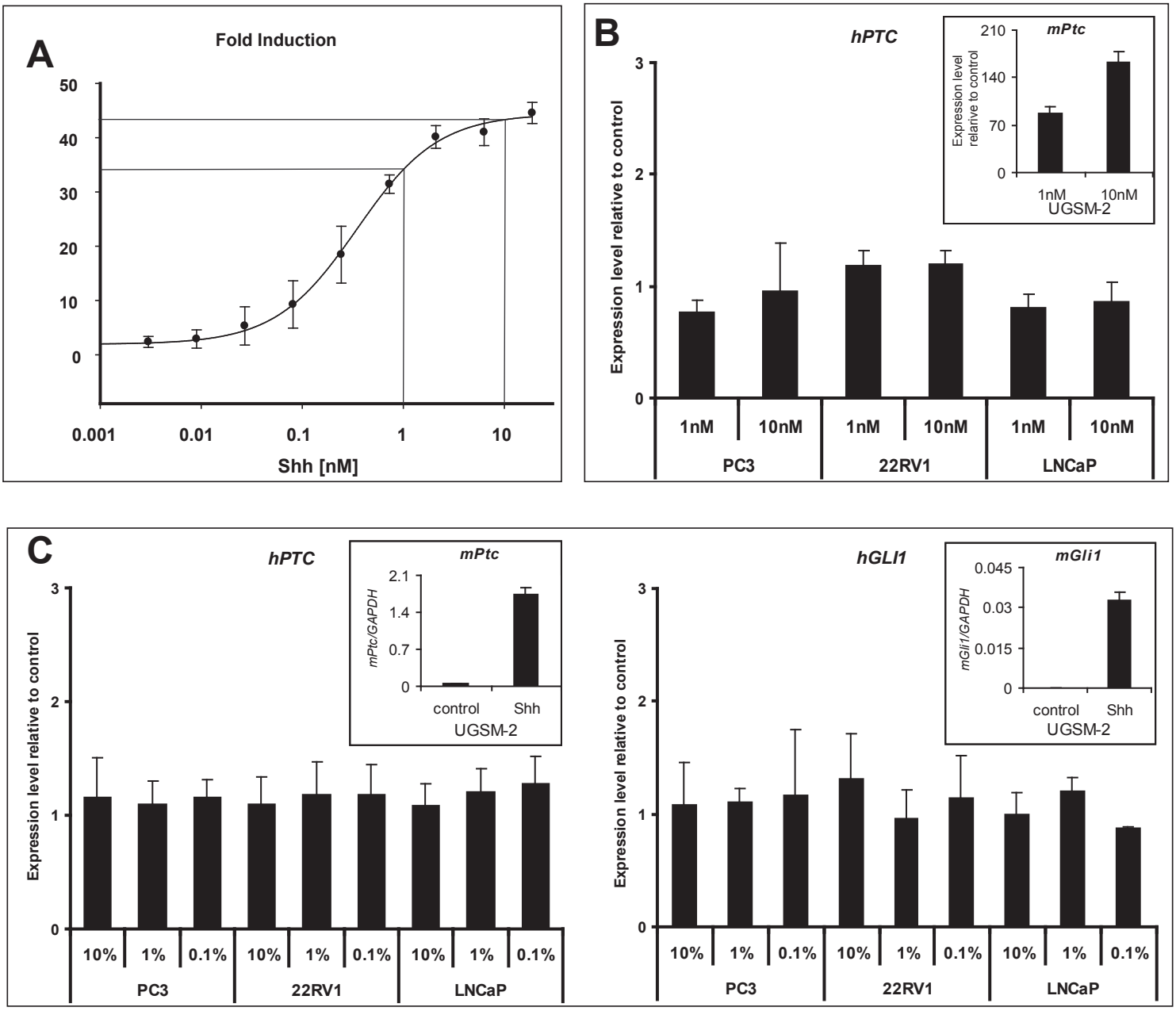

Figure 3 (A) Dose-response curve for Shh responsive Gli-luciferase reporter activity in NIH 3T3 cells. 1nM = EC75, 10nM = EC100. (B) Treatment of PC3, 22RV1 or LNCaP with 1nM or 10nM Shh does not increase Ptc expression. (C) Serum concentration does not alter Shh response of PC3, 22RV1 or LNCaP. However, 1 nM Shh is sufficient to significantly induce Ptc1 and Gli1 in UGSM-2 cells (1% FCS), $p<0.005$ (insert).

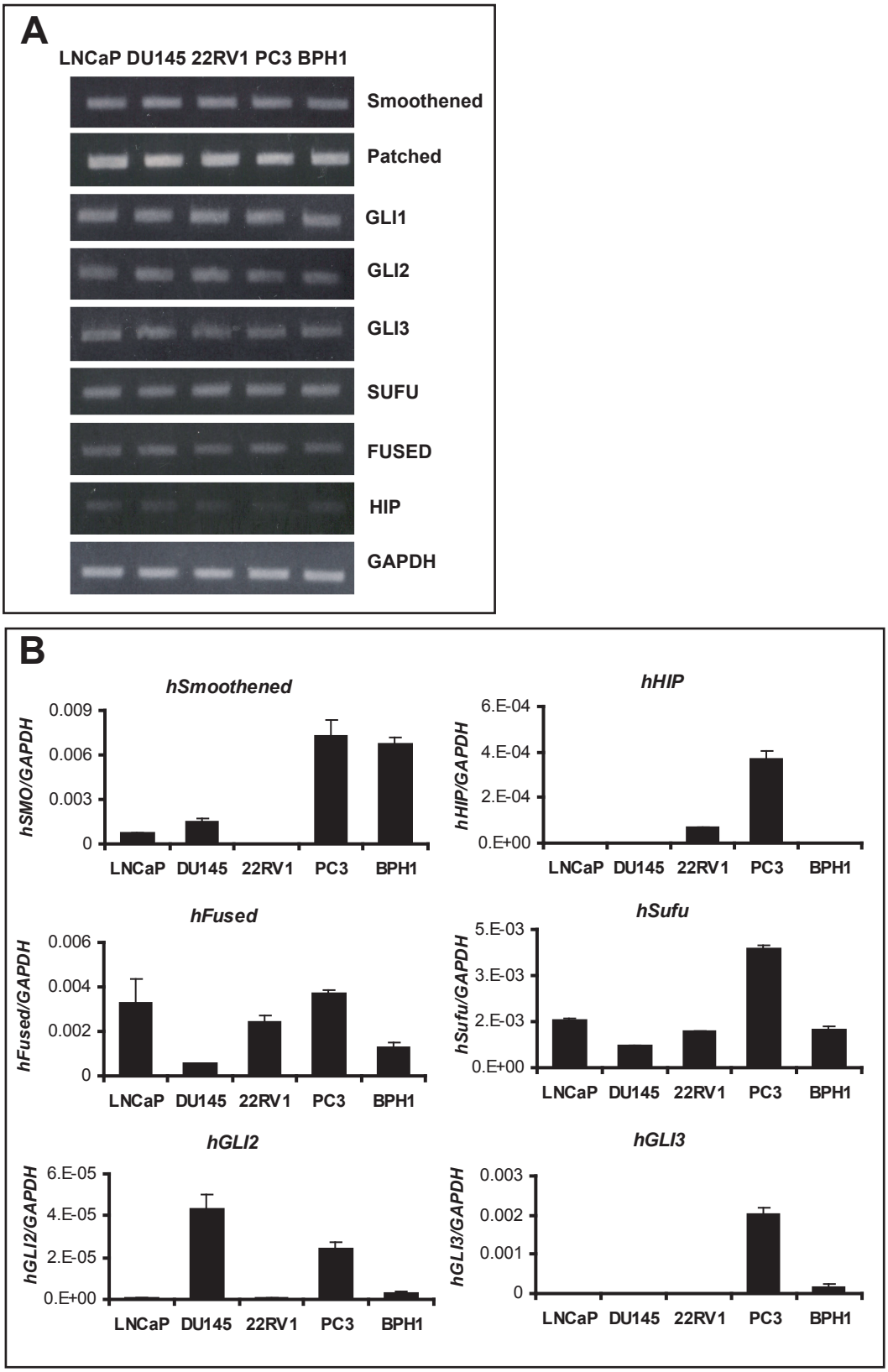

Figure 4 Expression of Hh pathway genes Smo, Ptc1, Gli1, Gli2, Gli3, SuFu, Fused and Hip in LNCaP, DU145, PC3, 22RV1 and BPH-1. (A) Resolution of RT-PCR products (40 cycles) on a 2% agarose gel using GAPDH as a loading control. (B) Quantitative real-time RT-PCR for the Hh pathway genes shows variations in the steady state levels of individual pathway components.

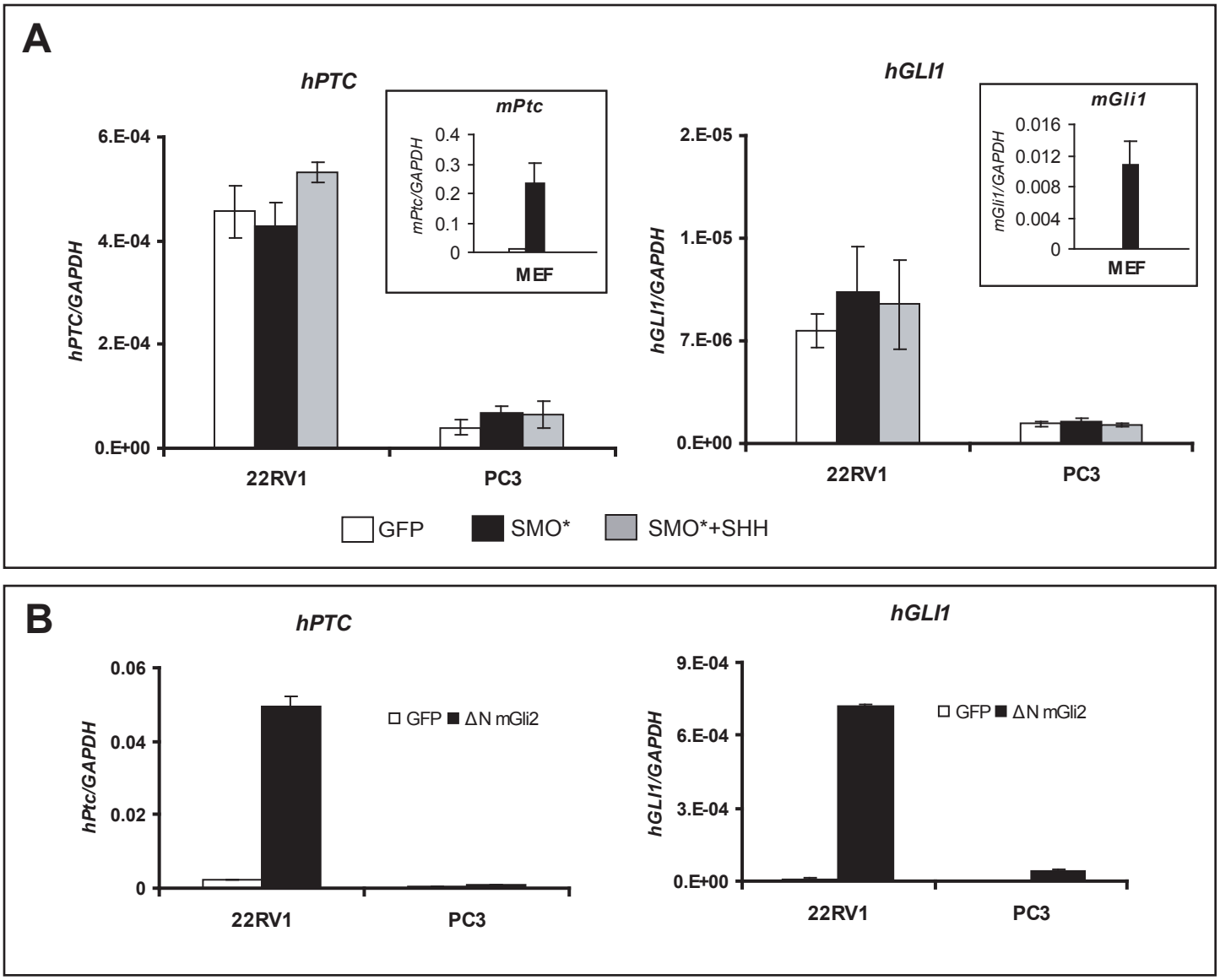

Figure 5 (A) Infection of PC3 and 22RV1 with a Smo* adenoviral vector did not activate expression of Hh target genes Ptc or Gli1, even when exogenous Shh was added. (insert A) Activation of Ptc1 and Gli1 is achieved in MEF cells under the same conditions ($p<0.05$). (B) Infection of PC3 and 22RV1 with a ΔNmGli2 adenoviral vector induced Hh target gene expression. Both PC3 and 22RV1 exhibit significant increases in Gli1 expression ($p<0.05$); Ptc expression was significantly increased in 22RV1 cells ($p<0.005$) but not in PC3 cells ($p=0.097$). Adenovirus infection rates for all constructs was ~90%.

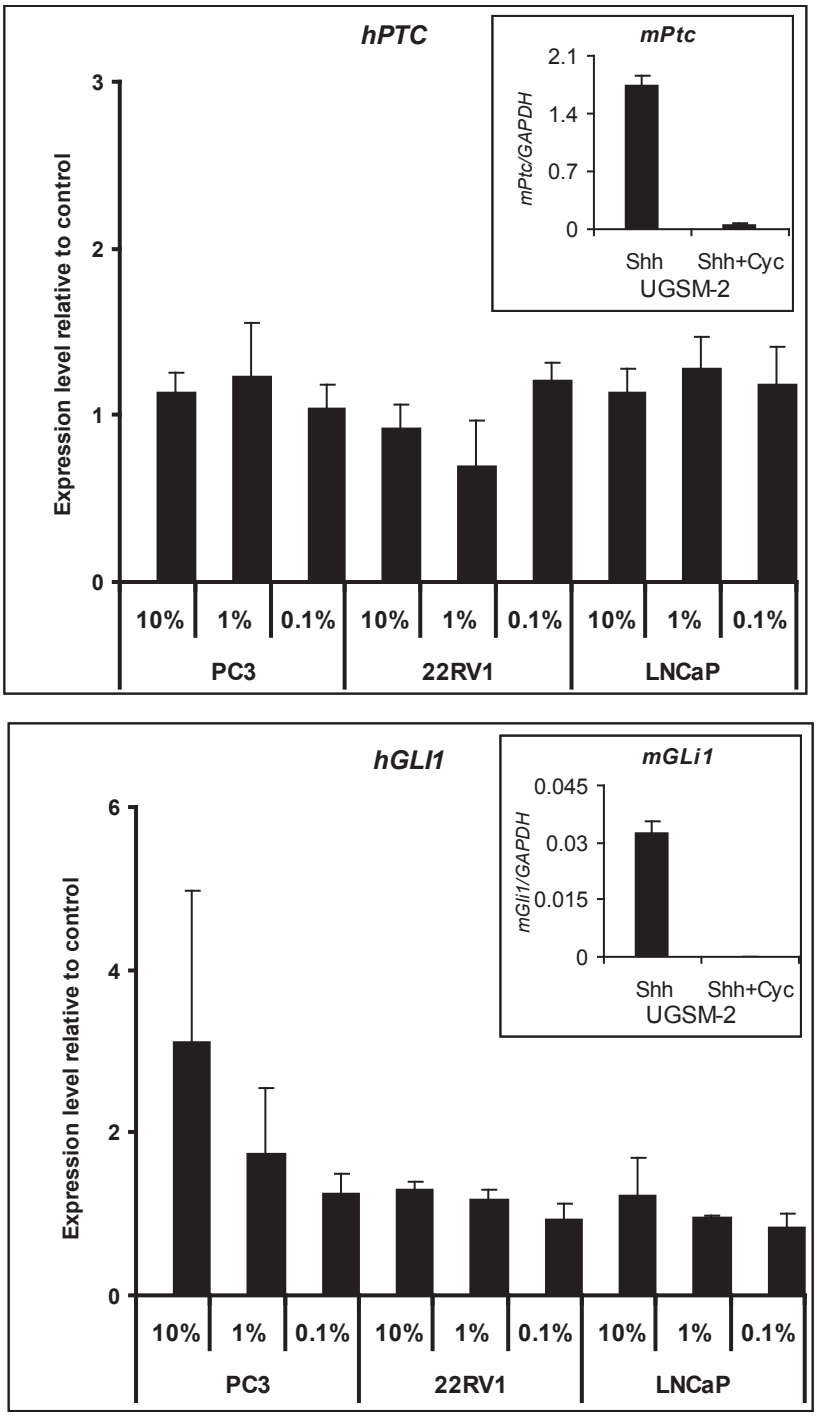

Figure 6 Cyclopamine (5 μM) treatment of PC3, 22RV1 and LNCaP cells in media supplemented with 10, 1, 0.1% FCS did not alter expression of the Hh target genes Ptc or Gli1. Target gene expression was induced by Shh and inhibited by 5uM cyclopamine in UGSM-2 cells $p<0.005$, (insert).

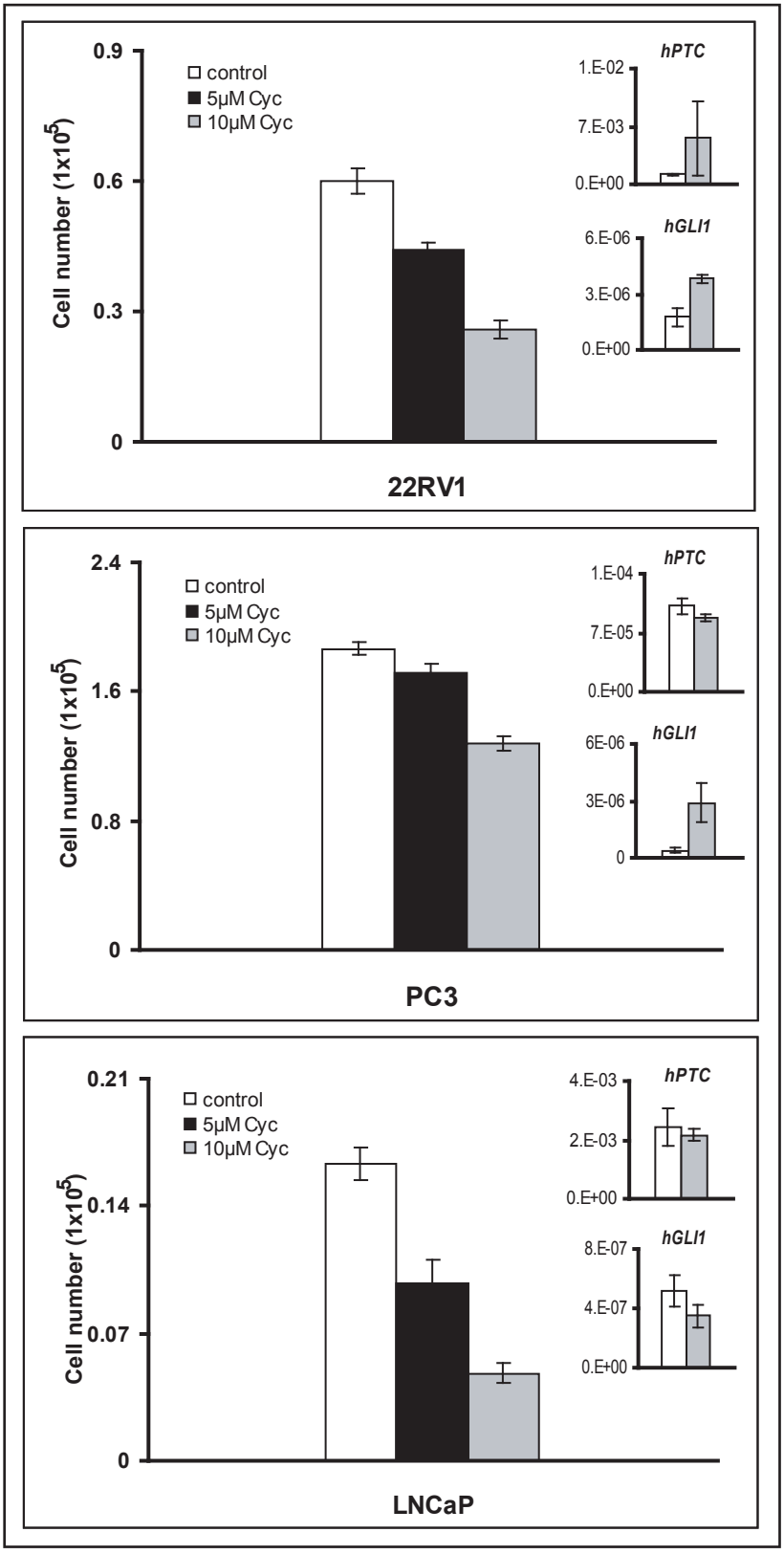

Figure 7 Proliferation of 22RV1, PC3, and LNCaP cells over 4 days was inhibited by cyclopamine in a dose dependent fashion ($p<0.05$ at 10uM cyclopamine). In these cultures expression of the Hh target genes Ptc and Gli1 were not altered by 10uM cyclopamine suggesting that the reduction in proliferation was not through a Smo-mediated event (insert).

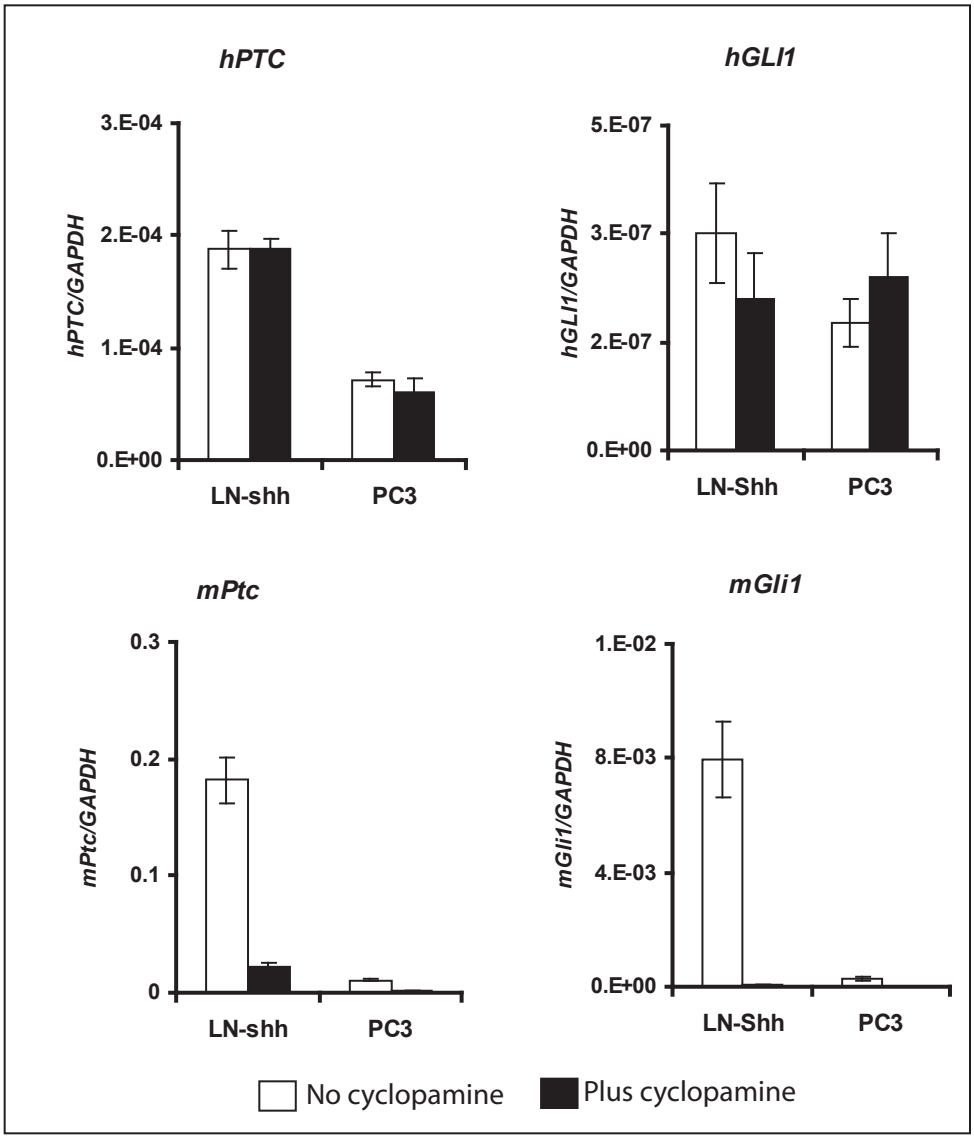

Figure 8 Effect of 10uM cyclopamine on autocrine and paracrine pathway activity in co-cultures of either LNCaP cells over-expressing Shh (LN-Shh) or PC3 cells co-cultured with mouse UGSM-2 cells. There is no effect on expression of hPtc and hGli1 (upper panel). However inhibition of paracrine signaling in UGSM-2 co-cultured with either LN-Shh or PC3 is evident from the decrease in mPtc and mGli1 expression in the presence of cyclopamine (lower panel; $p<0.05$).

EXPERIMENTAL CELL RESEARCH 312 (2006) 1925–1938

available at www.sciencedirect.com

SCIENCE DIRECT®

www.elsevier.com/locate/yexcr

Research Article

Unique and complimentary activities of the Gli transcription factors in Hedgehog signaling

Robert J. Lipinski[a,b], *Jerry J. Gipp*[b], *Jingxian Zhang*[b], *Jason D. Doles*[b], *Wade Bushman*[a,b,*]

[a]*Molecular and Environmental Toxicology Center, Madison, WI 53705-222, USA*
[b]*Department of Surgery, The University of Wisconsin-Madison, Madison, WI 53703, USA*

ARTICLE INFORMATION

Article Chronology:
Received 15 December 2005
Revised version received
15 February 2006
Accepted 22 February 2006
Available online 29 March 2006

Keywords:
Gli1
Gli2
Gli3
Sonic Hedgehog
Transcription factors
Mouse embryonic fibroblasts

ABSTRACT

The Gli family of transcription factors (Gli1, 2 and 3) mediate the Hedgehog morphogenetic signal by regulating the expression of downstream target genes. Aberrations in Hedgehog signaling seriously affect vertebrate development. Postnatally, Hedgehog signaling has been postulated to play a pivotal role in healing and repair processes and inappropriate pathway activation has been implicated in several types of cancers. To better understand both the upstream regulation of the Gli transcription factors, as well as their unique and combinatorial roles in regulating the expression of Hedgehog target genes, we have characterized embryonic fibroblasts (MEFs) from *Gli* mutant mice. Stimulation of wild-type MEFs by Sonic Hedgehog (Shh) peptide elicited unique profiles of induction of Hedgehog target genes *Gli1*, *Ptc1*, and *Hip1*. *Gli2* loss-of-function was associated with diminished Shh-induced target gene expression, while *Gli3* loss-of-function was associated with increased basal and Shh-induced target gene expression. The loss of *Gli1* alone had no effect on target gene induction but did diminish Shh-induced target gene expression when combined with the loss of *Gli2* or *Gli3*. Additionally, overexpression of *Gli1* induced target gene expression in *Gli2*$^{-/-}$*3*$^{-/-}$ MEFs, while Shh stimulation did not. Using MEFs expressing only *Gli2* or *Gli3*, we found that both cyclopamine and the PKA activator forskolin inhibited target gene induction mediated by Gli2 and Gli3. These results demonstrate that Gli2 and Gli3 share common regulatory mechanisms and modulate Hedgehog target gene expression directly and independently while also regulating *Gli1* expression, which in specific contexts, coordinately contributes to target gene activation.

Introduction

Hedgehog signaling is a conserved inductive signaling pathway that was first characterized in *Drosophila* and subsequently found to play profound roles in organogenesis and differentiation in a number of different vertebrate structures including the central nervous system, skeleton, lung, gut, and genitourinary system (reviewed in [1]). These studies have found a ready correlate in the study of teratogenic effects of disruptions in Hh signaling (reviewed in [2]). Hh signaling is generally diminished in the adult but recently, interest has surged in the apparent central role of Hh signaling in stem cell

* *Corresponding author*. Division of Urology, University of Wisconsin Medical School, K6/562 Clinical Science Center, 600 Highland Avenue, Madison, WI 53792, USA. Fax: +1 608 265 8133.
E-mail address: bushman@surgery.wisc.edu (W. Bushman).

0014-4827/$ – see front matter © 2006 Elsevier Inc. All rights reserved.
doi:10.1016/j.yexcr.2006.02.019

recruitment and proliferation, inflammation and healing, and tumor growth, progression, and metastasis (reviewed in [3]). The dramatic expansion in the context of Hh signaling has created an intense interest in the mechanics and regulation of Hh signaling among a wide audience working in fields distant from its well-studied niche of Hh in development. Going forward, it will be increasingly important to study the Hh signaling pathway at the cellular level and examine the regulatory mechanisms which regulate Hh signal transduction. Here we characterize, in a generalizable cell-based system, the individual and complementary contributions of the Gli family of transcriptional regulators in Hh-induced target gene activation.

Hedgehog (Hh) signaling is initiated when a Hedgehog ligand binds to a receptor Patched (Ptc) on the target cell and initiates an intracellular signal transduction cascade that results in changes in gene expression in the target cell. In vertebrates, the Gli family of transcription factors, Gli1, Gli2, and Gli3, mediates the Hh morphogenetic signal by regulating expression of Hh target genes. These three *Gli* genes share homology with the ancestral *Ci* gene of *Drosophila*, which encodes a zinc finger protein that mediates the transcriptional response to Hh stimulation. In the absence of Hh ligand, Ci is constitutively cleaved to a repressor protein that inhibits transcription of Hh target genes. In response to Hh stimulation, Ci proteolysis is blocked and the full-length form of the protein enters the nucleus to function as a transactivator of Hh target genes (reviewed in [1–4]).

The three vertebrate *Gli* genes have been postulated to subdivide the distinct features of Ci function into different moieties. Gli3 has retained several of the functional properties of Ci. Like Ci, Gli3 undergoes PKA-dependent proteolytic cleavage generating an N-terminal protein that preferentially accumulates in the nucleus and acts as a repressor of Hh target genes [5,6]. Hh stimulation prevents this processing and allows for the accumulation of full-length Gli3 [6,7]. Gli3 appears to function primarily as a repressor of gene expression and Gli3 loss-of-function is often functionally equated to overactivity of the Hh pathway. Although several investigations have found only a repressor function for Gli3 [6,8], it may also participate in the activation of Hh target genes [9,10]. It is unclear whether this activation is in collaboration with other Gli proteins, as a result of direct transactivating function, or as a consequence of de-repression.

Gli2 functions as an important transactivator of Hh signaling. Overexpression of *Gli2* in cell culture activates a *Gli* reporter construct [8] and induces Hh target genes in cultured presomitic mesoderm tissue [11]. Moreover, mouse embryos lacking functional Gli2 show diminished expression of conserved Hh targets *Gli1* and *Ptc1* [12,13]. The importance of Gli2 in mediating the Hh signal during vertebrate development is clear as *Gli2* homozygous null mice die prenatally and exhibit neural tube defects including a complete loss of the floor plate and a reduction in V3 interneurons [12,13]. Considerable uncertainty exists about the Hh-related upstream mechanisms regulating Gli2 activity. While a proteolytic cleavage of Gli2 is seen in transgenic *Drosophila* and in cultured cells [14], it is independent of Hh signaling and has not been demonstrated in any normal context. A role for Gli2 in repressing Hh target genes has also been suggested [11,15] but compelling evidence is lacking.

The role of Gli1 as a Hh target gene activator is evidenced by its ability to induce expression of Hh target genes when overexpressed in cell and tissue culture [7,11,15]. Upregulation of *Gli1* is a reliable marker of Hh signaling and overexpression of *Gli1* is a consistent hallmark of cancers with aberrant Hh pathway activation including basal cell carcinomas [16,17]. However, significant *Gli1* expression in normal cells is dependent upon Hh signaling activation, and it is therefore not thought to be the primary mediator of the Hh signal. Further, the dependence of normal development on intact Hh signaling contrasts with the observation that transgenic mice lacking the zinc finger DNA binding domain of *Gli1* are homozygous viable and fertile [18]. Gli1, like Ci, contains a zinc finger domain but does not appear to undergo proteolytic cleavage and there is no evidence for repressor activity.

The expansion of Ci-related functions to three separate Gli genes in the vertebrate has been postulated to allow for greater complexity in the regulatory apparatus. However, a comprehensive understanding of how the three Gli proteins work independently and coordinately to positively and negatively regulate the Hh signal in mammals has remained elusive. While the vast majority of these studies have been confined to the role of the *Gli* genes in a context of tissue development, a broader biological role of Hh signaling has recently been revealed in a range of fields including teratogenesis (reviewed in [2]), immune function (reviewed in [19]), tissue healing and repair [20,21], and childhood and adult tumor biology (Reviewed in [22]). Thus, the complexity of the Gli gene functional network not only subserves the intricate demands of vertebrate development but also likely accommodates more diverse and subspecialized roles of Hh signaling in other biological settings. Given the broadening importance of Hh signaling in a wide range of biological activities, there is an emerging need to examine the regulation of this pathway in a more generalizable context.

Mouse embryonic fibroblasts (MEFs) derived from transgenic knockout mice have been used extensively to characterize the role of numerous genes with diverse functions at the cellular level. To quantitatively describe upstream regulation of the individual Gli transcription factors and to assay their unique and combinatorial roles in regulating the expression of Hh target genes, we created and analyzed a complete set of embryonic fibroblasts (MEFs) from *Gli* mutant mice. This provided a tractable cell-based system in which to quantitatively examine the regulation of Hh target gene expression by the Gli transcription factors. Our studies use cell-based assays to test the many inferences made from the study of specific developmental models and ascertain their generalizability outside those specific contexts. More importantly, this quantitative analysis reveals unique kinetics of specific target gene activations and clarifies the unique and combinatorial actions of the three different Gli transcription factors in positively and negatively regulating Hh signaling at the cellular level as well as providing novel insight into upstream mechanisms that regulate the activity of each.

Materials and methods

MEF isolation

Dams were sacrificed at E13 and embryos were removed. For each cell type, all tissue remaining after removal of the liver and head region was passed through an 18 gauge syringe in 0.5 ml 0.25% trypsin. After incubating for 5 min at 37°C, tissue was pipetted up and down to produce single cells. MEFs were propagated in media with 10% fetal calf serum (FCS) (DMEM [with L-glutamine, 4.5 g/L glucose, without sodium pyruvate] with 1% Pen/Strep; 0.2% beta-mercaptoethanol) for 5 days and were then aliquoted, frozen, and stored in liquid nitrogen. *Gli1*$^{+/-}$ and *Gli2*$^{+/-}$ mice were generously provided by Alexandra Joyner and maintained on an outbred CD-1 background. *Gli3*$^{+/-}$ mice were obtained from Jackson Laboratories (Bar Harbor, ME) and were maintained on a C57/C3H background. Wild-type (WT) MEFs were harvested from strain appropriate wild-type embryos.

Cell treatment

Aliquoted cells were thawed and grown in 10% FCS (as described for MEF isolation) for 48 h. They were then trypsinized and plated in Multiwell Primaria™ 24 well plates (Falcon, Franklin Lakes, NJ) at 2.0×10^5 cells per well in 400 μl media. Cells were allowed to attach overnight and media were replaced with DMEM containing 1% FCS with the following; Shh-N peptide (R&D Systems, Minneapolis, MN) at 10 μg/ml, cyclopamine (Toronto Research Chemicals, Ontario, Canada) at 5 μM, or forskolin (LC Laboratories, Woburn, MA) at 50 μM. At indicated time points, RNA was harvested and gene expression was determined as described below.

Isolation of urogenital sinus-mesenchymal cells

Urogenital sinus mesenchymal (UGS-M) cells were isolated as described in Shaw et al. [23]. Cells were isolated from *Gli1*$^{-/-}$, *Gli2*$^{-/-}$, *Gli3*$^{-/-}$, and strain appropriate WT mice carrying homozygous *INK4a*$^{-/-}$ mutations. Experiments were performed using a nonclonal population of cells at passage 20 or less.

Adenovirus Infection

Adenovirus constructs carrying a mouse Gli1-GFP, mouse Gli2-GFP, or human Gli3-GFP fusion protein or GFP alone were generously provided by Chen-Ming Fan. Virus was produced as described [11]. MEFs were plated at confluence in media containing 10% FCS (as described for MEF isolation) and allowed to attach overnight. Media were replaced with DMEM containing 1% FCS +/− adenovirus at a concentration of 100 infectious units/cell. After 48 or 72 h incubation as stated in figure legends, RNA was harvested and gene expression was determined as described below. Under these conditions, 65% of MEFs were GFP positive by flow cytometry.

RNA isolation and Real Time-PCR

RNA was isolated at stated time points using Qiagen (Valencia, CA) RNeasy RNA isolation kits and subjected to on column DNase digestion. cDNA was generated from RNA by reverse transcription following standard protocols. Gene expression was assayed by Real Time RT-PCR using SYBR® Green PCR Master Mix (Applied Biosystems, Foster City, CA) on a Bio Rad (Hercules, CA) iCycler and normalized using the internal control gene *glyceraldehyde-3-phosphate dehydrogenase* (*GAPDH*). PCR reactions were run for 40 cycles. For Fig. 1A, PCR products were run on a 1.5% agarose gel. Gene-specific primer sequences used are as follows: *GAPDH*: 5′-AGCCTCGTCCCG TAGACAAAAT-3′ and 5′-CCGTGAGTG GAGTCATACTGGA-3′, *Shh*: 5′-AATGCC TTGGCCATCTCTGT-3′ and 5′-GCTCGA CCCTCATAGTGTAGAGAC T-3′, *Ptc1*: 5′-CTCTGGAGCAGATTTCCAAGG-3′ and 5′-TGCCGCAGTTCTTTTGAATG-3′, *Ptc2*: 5′-TCTCCAGCTTCTGACCCACT-3′ and 5′-GTCCCCTCCTCCTGACTGA-3′, *Smo*: 5′-TTGTGCTCATCACCTTCAGC-3′ and 5′-TGGCTTGGCATAGCACATAG-3′, *Gli1*: 5′-GGAAGTCCTATTCACGCCTTGA-3′ and 5′-CAACCTTCTTGCTCACACATG TAAG-3′, *Gli2*: 5′-CCTTCTCCAATGCCT CAGAC-3′ and 5′-GGGGTCTGTGTACCT CTTGG-3′, *Gli3*: 5′-AGCCCAAGTATTATT CAGAACCTTTC-3′ and 5′-ATGGATAGG GATTGGGAATGG-3′, *Hip1*: 5′-CCTGTC GAGGCTACTTTTCG-3′ and 5′-TCCATT GTGAGTCTGGGTCA-3′.

Statistical analysis, curve fitting, and expression normalization

For the time course experiment, to determine whether gene expression was significantly changed, a 95% confidence interval was calculated based on the mean and standard deviation of the observations. Changes reported as significant thus have a P value of <0.05. To test whether basal and Shh-induced target gene expression preserved the ordering implicitly suggested by the genotypes, a Jonckheere–Terpstra test was performed using Mstat version 4.01 (available at: http://macardle.oncology.wisc.edu/mstat). Student's t tests, paired t tests, and R^2 values were generated using SigmaPlot v. 9.0. To accommodate slight differences in the WT target gene expression levels between *Gli2*$^{-/-}$ and *Gli1*$^{-/-}$*2*$^{-/-}$ MEFs, and *Gli3*$^{-/-}$ and *Gli1*$^{-/-}$*3*$^{-/-}$ MEFs, we normalized the gene expression in mutant MEFs by dividing the basal and Shh-induced expression of Ptc1 and Hip1 by the expression in appropriate WT MEFs (Figs. 2B and 3B). Ratios were plotted on a semi-log scale where values less than one indicate a decrease in expression and values greater than one indicate an increase in expression in mutant MEFs relative to WT.

Results

Unique kinetics of Gli1 and Ptc1 vs. Hip1 induction

We first isolated wild-type (WT) MEFs from the embryonic day 13 (E13) WT embryo and assayed the expression of multiple genes integral for the Hh signaling pathway in the presence or absence of Shh peptide. While *Shh* itself was

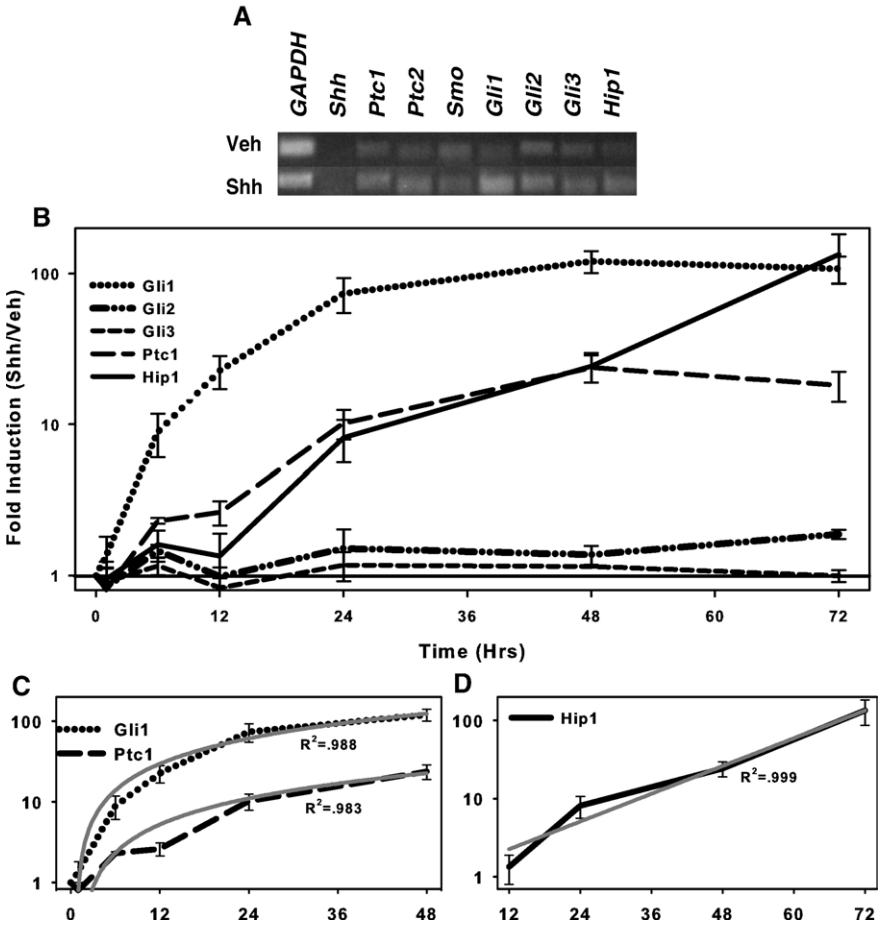

Fig. 1 – Unique kinetics of *Gli1* and *Ptc1* vs. *Hip1* induction. WT MEFs were plated at confluence and treated ± 10 μg/ml Shh-N peptide. At indicated time points, gene expression was determined by real-time RT-PCR. (A) At 48 h, Hh signaling genes *Ptc1*, *Ptc2*, *Smo*, *Gli1*, *Gli2*, *Gli3*, and *Hip1* but not *Shh* were expressed with or without Shh stimulation. (B) Semi-log plot showing Shh-stimulated fold induction of *Ptc1*, *Gli1*, *Gli2*, *Gli3*, and *Hip1* expression over time. (C) Between 0 and 48 h, *Gli1* and *Ptc1* induction follows a linear curve fit (R^2 = 0.988 and 0.983, respectively). (D) Between 12 and 72 h, *Hip1* induction fits an exponential-growth curve (R^2 = 0.999). Values represent the mean ± SEM of four replicate experiments.

not detectable, all other pathway genes assayed – *Ptc1*, *Ptc2*, *Smo*, *Gli1*, *Gli2*, *Gli3*, and *Hip1* – were expressed under both conditions (Fig. 1A). We then quantitatively characterized the transcriptional response of WT MEFs to stimulation by Shh peptide over a 72 h time course. Both *Gli1* and *Ptc1* exhibited a significant increase in expression as early as 6 h post Shh-stimulation (Fig. 1B). Expression continued to increase until it plateaued after 48 h. Analysis of *Gli1* and *Ptc1* expression curves showed a linear-like curve of induction (Fig. 1C). *Gli2* expression, which is not thought to be primarily regulated by Hh signaling was not significantly changed by 48 h, but did show a slight (< twofold) but significant induction at 72 h. While some evidence indicates that expression of *Gli3* is repressed by Hh signaling [24], it is thought to be primarily regulated at the protein level. We found no Shh-mediated change in *Gli3* expression over the 72-h time course. Hedgehog Interacting Protein (Hip1) is a cell surface protein that binds Hh peptides and is thought to function as part of a negative feedback loop that extinguishes the Hh signal [25]. *Hip1* expression was not significantly induced by 12 h, but was significantly induced by 24 h. Between 12 and 72 h, expression increased in an exponential-like fashion (Fig. 1D). These data show that the timing and kinetics of *Gli1* and *Ptc1* vs. *Hip1* induction differ.

Loss of Gli2 diminishes Shh-induced target gene expression

To assess the individual and combinatorial roles of the three Gli proteins in mediating Hh-induced target gene expression, we assayed the basal and Shh-induced expression of *Gli1*, *Ptc1*, and *Hip1* in E13 *Gli*-mutant MEFs treated +/– Shh-N peptide for 48 h (Fig. 2A). We first tested whether an association existed between *Gli* gene dosage (e.g. $Gli1^{+/+}$ vs. $Gli1^{+/-}$ vs. $Gli1^{-/-}$) and the basal or Shh-induced expression of each target gene. We utilized the Jonckheere–Terpstra test, which is a nonparametric test for ordered differences among classes. The loss of *Gli1* alleles was associated with a slight increase in the basal expression of *Ptc1* and *Hip1* (P = 0.096 and P = 0.035, respectively) (Jonckheere–Terpstra test) but the differences were less than twofold. No effect of *Gli1* loss-of-function on Shh-induced *Ptc1* and *Hip1* expression was observed (P = 0.91

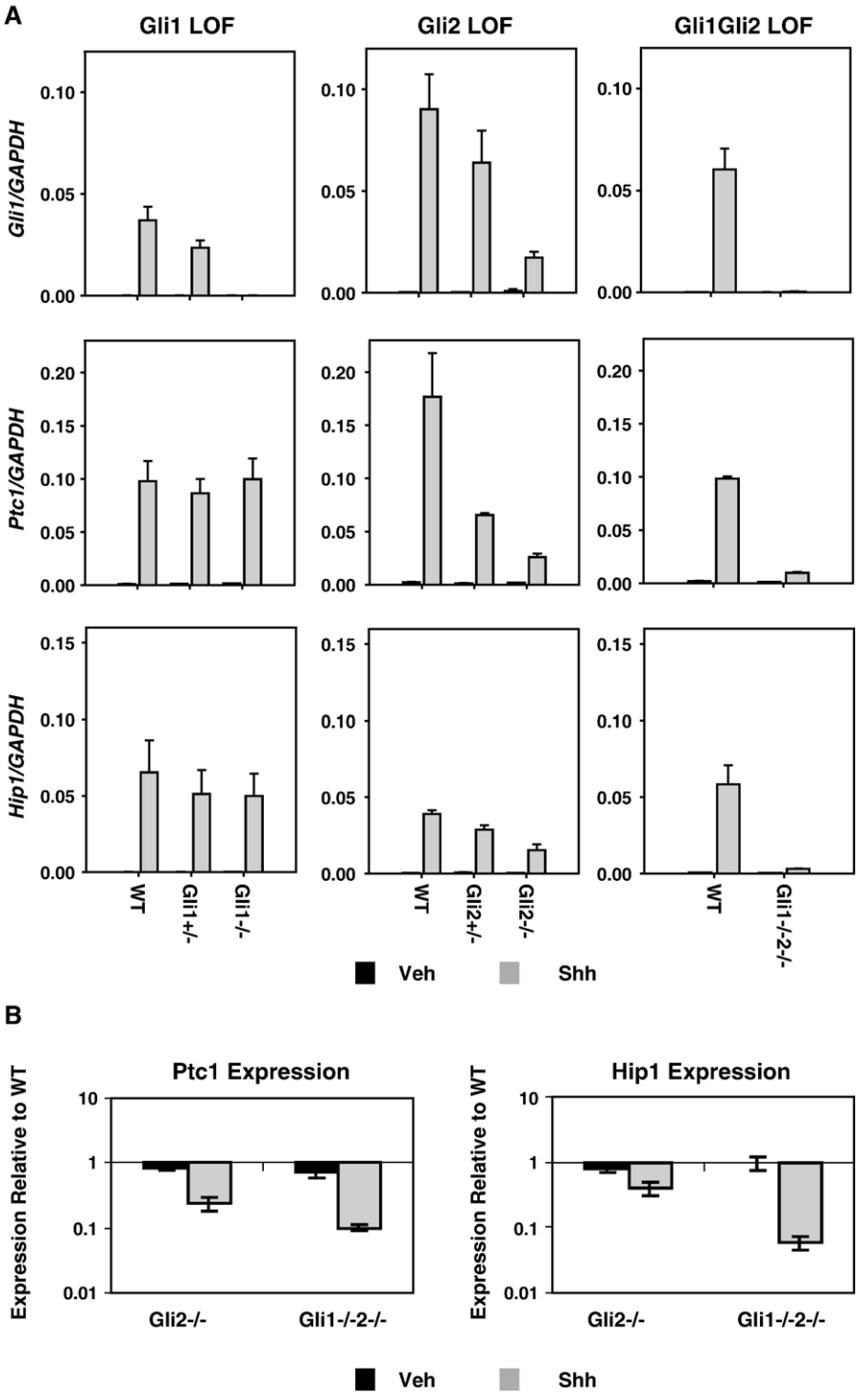

Fig. 2 – Loss of *Gli2* diminishes Shh-induced target gene expression. (A) *Gli1*$^{+/-}$, *Gli1*$^{-/-}$, *Gli2*$^{+/-}$, *Gli2*$^{-/-}$, *Gli1*$^{-/-}$*2*$^{-/-}$, and strain appropriate WT MEFs were plated at confluence and treated ± 10 μg/ml Shh-N peptide. After 48 h, expression of *Gli1*, *Ptc1*, and *Hip1* was determined by real-time RT-PCR. Values represent the mean ± SEM of three replicate experiments. (B) The ratio of basal and Shh-induced expression of *Ptc1* and *Hip1* in *Gli2*$^{-/-}$ and *Gli1*$^{-/-}$*2*$^{-/-}$ MEFs relative to respective WT expression values. On this semi-log plot, values less than one indicate a decrease in expression and values greater than one indicate an increase in expression in the mutant MEFs relative to WT.

and 0.22). The loss of *Gli2* alleles had no significant effect on the basal expression of *Gli1*, *Ptc1*, or *Hip1* ($P = 0.15$, $P = 0.74$, $P = 0.31$). However, decreased Shh-induced *Gli1*, *Ptc1*, and *Hip1* expression was significantly associated with the dose-dependent loss of *Gli2* alleles ($P = 0.0055$, $P = 0.0027$, $P = 0.0027$). Expression of *Gli2* in *Gli2*$^{+/-}$ MEFs was reduced compared to *Gli2*$^{+/+}$ MEFs in both the basal and Shh stimulated states (35 ± 6% and 62 ± 19%, respectively). This

implicates Gli2 as a key positive regulator of Shh-induced target gene expression and suggests that *Gli2*$^{+/-}$ MEFs are haploinsufficient in Hh target gene induction.

Gli1 transgenic null mice are phenotypically normal, but mice with combined loss of *Gli1* and *Gli2* function have more severe phenotypes than those with *Gli2* loss-of-function alone [18]. This has been taken to suggest that an unequal functional redundancy exists between Gli1 and Gli2. To examine whether this functional redundancy is evident at the level of the transcriptional response of MEFs to Shh stimulation, we assayed the effect of combined *Gli1* and *Gli2* loss of function. Shh stimulation increased *Ptc1* and *Hip1* expression in *Gli1*$^{-/-}$*2*$^{-/-}$ MEFs ($P = 0.0097$ and $P = 0.0072$, respectively, paired *t* test) (Fig. 2A). To determine how the combined loss of *Gli1* and *Gli2* affected basal and induced gene expression, we compared the basal and Shh-induced expression levels of *Ptc1* and *Hip1* in *Gli2*$^{-/-}$ and *Gli1*$^{-/-}$*2*$^{-/-}$ MEFs relative to WT values in semi-log plots (Fig. 2B). When *Gli1/Gli2* combined loss-of-function [*Gli1*$^{-/-}$*2*$^{-/-}$] was compared to *Gli2* loss-of-function alone, basal expression was not significantly affected but the Shh-induced expression *Ptc1* was impaired ($P = 0.021$ *t* test). This suggests that both *Gli1* and *Gli2* contribute to Shh-stimulated target gene activation. Combined with analysis of single *Gli1* and *Gli2* homozygous-null mutations, it suggests that complete functional compensation occurs in the absence of *Gli1*, but that incomplete compensation attends loss of *Gli2* function.

Loss of Gli3 increases basal and Shh-induced target gene expression

The basal expression of *Gli1*, *Ptc1*, and *Hip1* was positively associated with the loss of *Gli3* alleles ($P = 0.011$, $P = 0.0027$, $P = 0.0023$, Jonckheere–Terpstra) (Fig. 3A). Shh-induced expression of these three target genes was also dose-dependently associated with the loss of *Gli3* alleles ($P = 0.020$, $P = 0.035$, $P = 0.0037$). These findings implicate Gli3 as a repressor of Hh target gene expression. This is evident in both the basal and Shh-induced states.

Relative to WT controls, *Gli1*$^{-/-}$*3*$^{-/-}$ MEFs exhibited higher basal expression of *Ptc1* and *Hip1* ($P = 0.015$, 0.010 paired *t* test) similar to what was observed in *Gli3*$^{-/-}$ MEFs (Fig. 3A). Shh treatment resulted in a significant increase in the expression of both *Ptc1* and *Hip1* ($P = 0.013$ and $P = 0.0029$, respectively, paired *t* test). Whereas the *Gli3*$^{-/-}$ MEFs exhibited an induction of *Ptc1* and *Hip1* that greatly exceeded the maximal expression observed in the WT MEFs, this was not seen in *Gli1*$^{-/-}$*Gli3*$^{-/-}$ MEFs. To directly relate *Gli3*$^{-/-}$ and *Gli1*$^{-/-}$*3*$^{-/-}$ MEFs, we compared the basal and Shh-induced expression of *Ptc1* and *Hip1* in *Gli3*$^{-/-}$ and *Gli1*$^{-/-}$*3*$^{-/-}$ MEFs relative to WT values on semi-log plots (Fig. 3B). These data show a comparable increase in the basal levels of *Ptc1* and *Hip1* expression in the *Gli3*$^{-/-}$ and *Gli1*$^{-/-}$*3*$^{-/-}$ MEFs. However, the induction of *Ptc1* and *Hip1* in *Gli1*$^{-/-}$*3*$^{-/-}$ MEFs is severely reduced compared to *Gli3*$^{-/-}$ MEFs ($P = 0.0029$ and $P = 0.0069$, respectively) (Fig. 3B). This demonstrates that the exaggerated induction of *Ptc1* and *Hip1* in *Gli3*$^{-/-}$ MEFs depends upon the activity of Gli1.

Hh signaling defects in Gli2$^{-/-}$ *and Gli3*$^{-/-}$ *MEFs can be rescued by expression of Gli2 and Gli3*

Analysis of Gli LOF in developing animals and tissues may be complicated by the chronic deficiency prior to analysis. Similarly, in this study, MEFs were isolated from the context of chronic Gli LOF in vivo and then further propagated in vitro. Over time, the chronic absence of Gli function may trigger compensation mechanisms or other changes that alter the Hh responsiveness of the cell or tissue. To investigate this question, we overexpressed *Gli2* or *Gli3* in *Gli2*$^{-/-}$ and *Gli3*$^{-/-}$ MEFs by adenovirus infection. Expression of *Gli2* in *Gli2*$^{-/-}$ MEFs caused a minimal increase in basal *Gli1* expression and restored Shh stimulated activation of *Gli1*, to the level seen in Shh stimulated WT MEFs (Fig. 4A). Additionally, expression of *Gli3* reduced the elevated basal expression of *Gli1* seen in *Gli3*$^{-/-}$ MEFs (Fig. 4B). *Ptc1* and *Hip1* expression patterns mimicked that of *Gli1* in both rescue experiments (data not shown). These experiments indicate that the Hh signaling defects in *Gli2*$^{-/-}$ and *Gli3*$^{-/-}$ MEFs are not due to fixed compensatory mechanisms or other secondary effects of chronic Gli loss of function.

Loss of Gli2 and Gli3 prevents target gene induction by Shh

Gli2$^{-/-}$*3*$^{-/-}$ MEFs exhibited increased basal expression of *Ptc1* and *Hip1* relative to WT MEFs ($P = 0.0013$ and $P = 0.0070$ paired *t* test) (Fig. 5). However, no induction of either *Ptc1* or *Hip1* expression occurred with Shh stimulation. The inability of cells lacking *Gli2* and *Gli3* to induce Hh target genes mirrors the findings of Buttitta et al. [11] and McDermott et al. [26] in studies of Hh signaling in skeletal muscle formation. Taken in combination, the responses of the *Gli1*$^{-/-}$*3*$^{-/-}$ MEFs and *Gli2*$^{-/-}$*3*$^{-/-}$ MEFs indicates that Gli2 alone is sufficient to mediate target gene activation in response to Shh stimulation but that Gli1 is not. This could signify that Gli1 is unable to mediate target gene transactivation in the absence of Gli2 and Gli3. Alternatively, it could simply reflect a dependence of Gli1-mediated gene activation on the upregulation of *Gli1* expression that does not occur in the absence of Gli2 and Gli3.

Gli1 can activate target gene expression in the absence of Gli2 and Gli3

We infected WT and *Gli2*$^{-/-}$*3*$^{-/-}$ MEFs with adenovirus encoding a mouse Gli1-GFP fusion protein or GFP alone [11]. Infection of WT MEFs with Gli1-GFP encoding virus achieved *Gli1* expression comparable to the level induced by Shh peptide (Fig. 6). While this was sufficient to significantly induce both *Ptc1* and *Hip1* ($P = 0.038$ and $P = 0.045$, respectively, paired *t* test), the expression of both was significantly reduced compared to Shh-induced levels ($P = 0.0015$ and $P = 0.015$, respectively). Further, overexpression of *Gli1* was also capable of inducing both *Ptc1* and *Hip1* ($P = 0.0031$ and $P = 0.012$, respectively) in *Gli2*$^{-/-}$*3*$^{-/-}$ MEFs. This indicates that Gli1 can mediate target gene transactivation in the absence of Gli2 and Gli3 and suggests that the absence of any Shh-induced target gene induction in the *Gli2*$^{-/-}$*3*$^{-/-}$ MEFs results primarily from a failure of *Gli1*

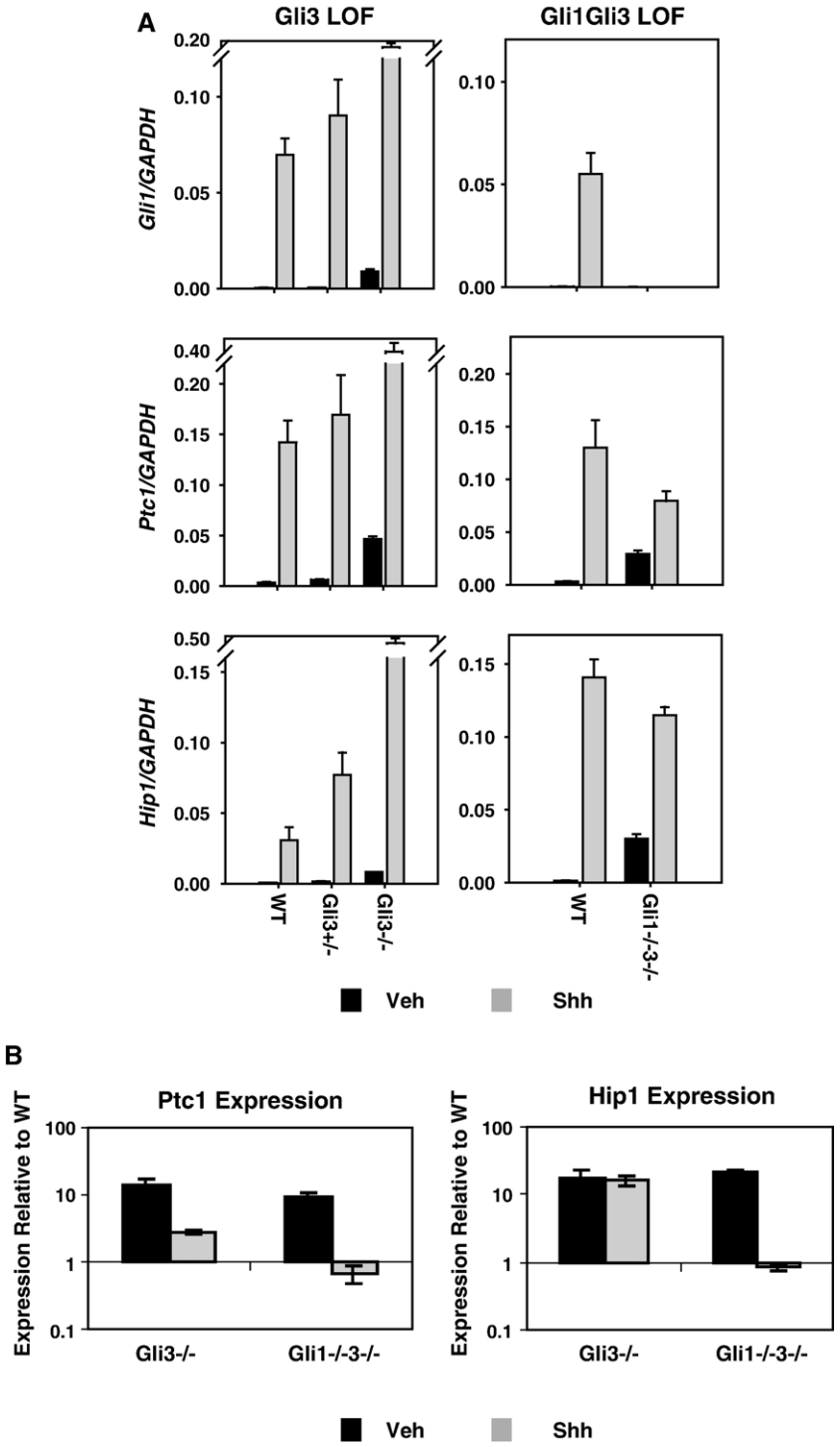

Fig. 3 – Loss of *Gli3* increases basal and Shh-induced target gene expression. (A) *Gli3*$^{+/-}$, *Gli3*$^{-/-}$, *Gli1*$^{-/-}$*3*$^{-/-}$, and strain-appropriate WT MEFs were plated at confluence and treated ± 10 μg/ml Shh-N peptide. After 48 h, expression of *Gli1*, *Ptc1*, and *Hip1* was determined by real-time RT-PCR. Values represent the mean ± SEM of three replicate experiments. (B) The ratio of basal and Shh-induced expression of *Ptc1* and *Hip1* in *Gli3*$^{-/-}$ and *Gli1*$^{-/-}$*3*$^{-/-}$ MEFs relative to respective WT values. Values below one indicate a decrease in expression and values greater than one indicate an increase in expression in the mutant MEFs relative to WT.

expression to increase following Shh stimulation. To determine whether Shh stimulation affected the ability of Gli1 to induce *Ptc1* and *Hip1* in the absence of Gli2 and Gli3, we overexpressed *Gli1* by adenovirus infection in *Gli2*$^{-/-}$*3*$^{-/-}$ MEFs and simultaneously stimulated with Shh peptide. The addition of Shh peptide did not alter the induction of *Ptc1* and *Hip1* by *Gli1* overexpression (data not shown).

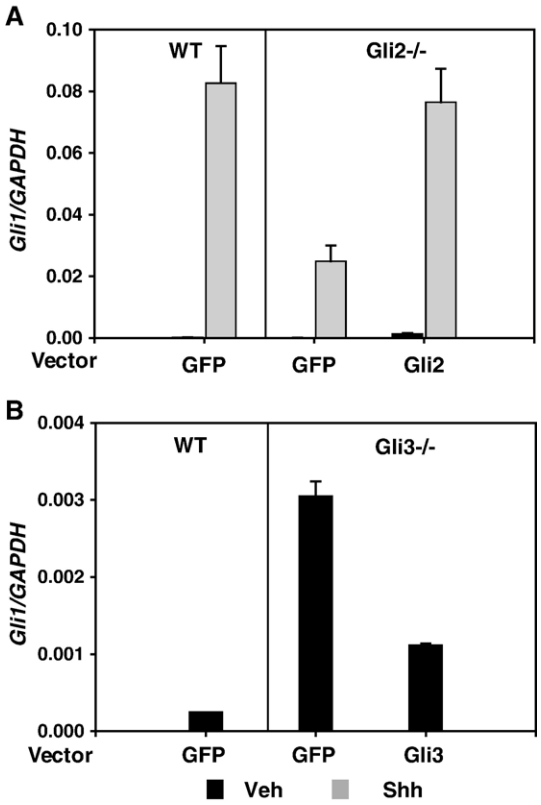

Fig. 4 – Hh signaling defects in *Gli2*$^{-/-}$ and *Gli3*$^{-/-}$ MEFs can be rescued by expression of Gli2 and Gli3. (A) WT and *Gli2*$^{-/-}$ MEFs were infected with adenovirus encoding a mouse Gli2-GFP fusion protein or GFP alone and treated ± 10 μg/ml Shh-N. (B) WT and *Gli3*$^{-/-}$ MEFs were infected with adenovirus encoding a human Gli3-GFP fusion protein or GFP alone. After 48 (A) or 72 (B) h, expression of *Gli1* was determined by real-time RT-PCR. Values represent the mean ± SEM of three replicate experiments.

Gli LOF in tissue-specific urogenital sinus mesenchyme cells mimics Hh signaling alterations in MEFs

Intact Hh signaling is required for proper prostatic budding, ductal growth, and branching [27–30]. We have previously shown that Shh from the epithelium of the urogenital sinus (UGS) induces *Gli1* in the surrounding UGS mesenchyme, which also expresses *Gli2* and *Gli3* [31]. To assess whether our analysis of *Gli* gene LOF in a heterogeneous MEF cell population corresponds to the effects of *Gli* gene LOF in tissue-specific cells, we isolated mesenchyme cells from the urogenital sinus of *Gli1*$^{-/-}$, *Gli2*$^{-/-}$, *Gli3*$^{-/-}$, and appropriate WT mice. These mice were crossed with INK4a$^{-/-}$ mice, allowing for immortalization of each cell line. Each urogenital sinus-mesenchymal (UGS-M) cell line was then treated +/− Shh peptide under conditions similar to MEF assays. We found that while *Gli1* LOF did not alter Shh stimulated induction of *Ptc1* (data not shown), the Shh stimulated expression of *Gli1* and *Ptc1* was markedly reduced in *Gli2*$^{-/-}$ UGS-M cells (Fig. 7). Furthermore, in *Gli3*$^{-/-}$ UGS-M cells, the basal and Shh-induced expression of *Gli1* and *Ptc1* was markedly increased over WT levels (Fig. 7).

Gli2 and Gli3 exhibit common regulatory mechanisms

Gli1 appears to be primarily regulated at the level of transcription, as its expression depends upon positive Hh signaling. Here, we found that *Gli1* expression is regulated by both Gli2 and Gli3 and that Shh stimulation does not affect *Gli1* function in the absence of Gli2 and Gli3. Conversely, the expression of neither *Gli2* nor *Gli3* is dramatically changed by Hh signaling and it has been assumed that regulation of target gene expression by Gli2 and/or Gli3 involves changes in protein phosphorylation, cleavage, or localization. Here, we found that MEFs singly expressing Gli2 or Gli3 transcriptionally respond to

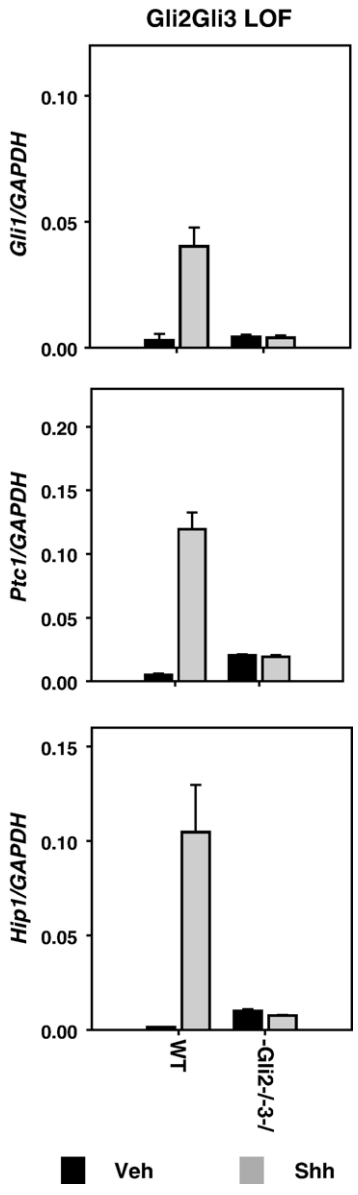

Fig. 5 – Loss of *Gli2* and *Gli3* prevents target gene induction by Shh-stimulation. *Gli2*$^{-/-}$*3*$^{-/-}$ and strain-appropriate WT MEFs were plated at confluence and treated ± 10 μg/ml Shh-N peptide. After 48 h, expression of *Gli1*, *Ptc1*, and *Hip1* was determined by real-time RT-PCR. Values represent the mean ± SEM of three replicate experiments.

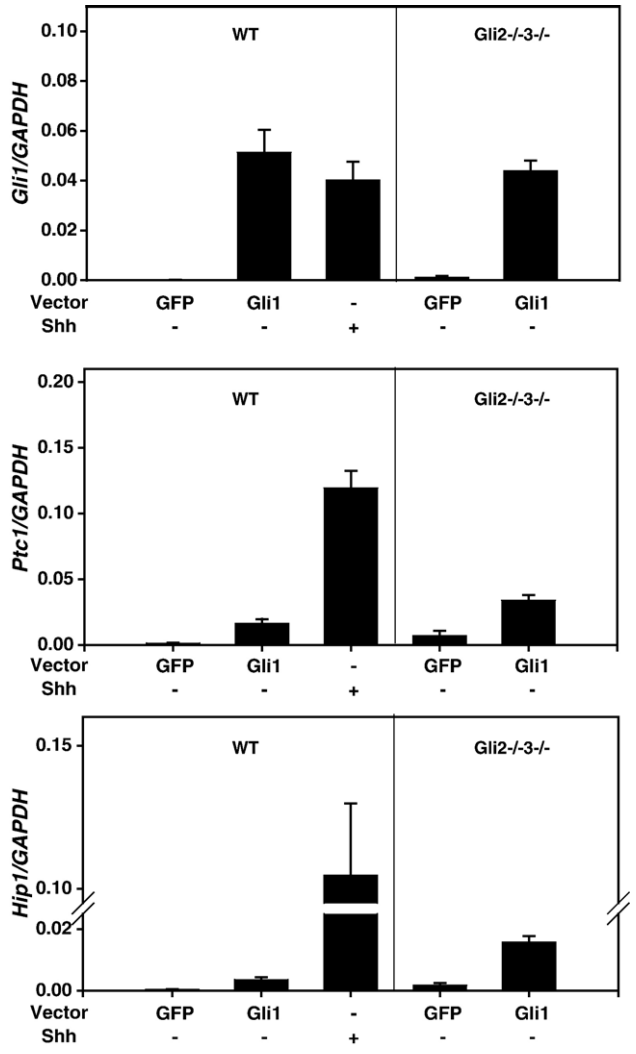

Fig. 6 – Gli1 can activate target gene expression in the absence of *Gli2* and *Gli3*. WT and *Gli2*$^{-/-}$*3*$^{-/-}$ MEFs were infected with adenovirus encoding a mouse Gli1-GFP fusion protein or GFP alone. After 48 h, expression of *Gli1*, *Ptc1*, and *Hip1* was determined by real-time RT-PCR. Values represent the mean ± SEM of three replicate experiments.

Shh ligand, enabling us to study mechanisms regulating each in isolation.

Cyclopamine is a teratogenic plant steroidal alkaloid, which acts by blocking Hh signaling. It has been shown to block Hh target gene induction in several in vitro and in vivo models [32,33], acting at the level of Smoothened [45]. Treating WT, *Gli1*$^{-/-}$*2*$^{-/-}$, and *Gli1*$^{-/-}$*3*$^{-/-}$ MEFs with Shh in the presence or absence of cyclopamine, we found that cyclopamine potently blocked Shh-stimulated target gene induction by both Gli2 and Gli3 (Fig. 8A). Interestingly, cyclopamine did not significantly affect the elevated basal target gene expression in cells expressing only Gli2. This is consistent with the recent observation that cyclopamine does not abolish Gli1 expression in embryonic kidneys from *Gli3*$^{-/-}$ mice cultured in vitro [34].

cAMP-dependent protein kinase (PKA) acts as a negative regulator of Hh signaling [35–37] and forskolin, an activator of adenylate cyclase, has also been shown to antagonize Hh signaling [33,38,39]. Forskolin treatment blocked *Ptc1* induction in WT and *Gli1*$^{-/-}$*2*$^{-/-}$ MEFs. In *Gli1*$^{-/-}$*3*$^{-/-}$ MEFs, forskolin treatment lowered the basal and Shh-induced expression of *Ptc1* ($P = 0.015$ and $P = 0.053$, respectively) resulting in a 55% reduction in its induction compared to WT cells (Fig. 8B). These results suggest that Hh signaling regulates the activity of Gli2 and Gli3 by mechanisms that share sensitivity to cyclopamine and forskolin.

Discussion

Primary mouse embryonic fibroblasts responded to Shh stimulation with the induction of Hh target genes *Gli1*, *Ptc1*, and *Hip1*. The time course of gene expression following Shh treatment of WT MEFs revealed unique kinetic profiles of target gene induction (Fig. 1). This unexpected difference in the kinetics of gene induction may explain a previously noted offset in *Gli1* and *Hip1* activation [40] and suggests a feature of target gene regulation that may have important functional consequences. Hip1 was first identified as a membrane glycoprotein capable of binding all three Hh ligands [25]. *Hip1* expression is induced in the presence of Hh ligand and has

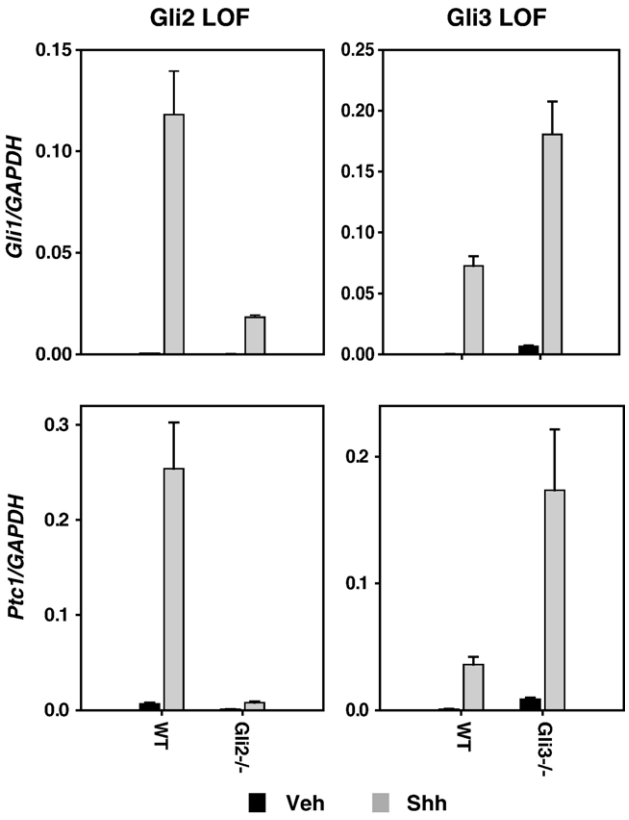

Fig. 7 – Gli LOF in tissue-specific urogenital sinus mesenchyme cells mimics Hh signaling alterations in MEFs. *Gli2*$^{-/-}$, *Gli3*$^{-/-}$, and strain appropriate WT urogenital sinus mesenchyme cells were plated at confluence and treated ± 10 μg/ml Shh-N peptide. After 48 h, expression of *Gli1* and *Ptc1* was determined by real-time RT-PCR. Values represent the mean ± SEM of three replicate experiments.

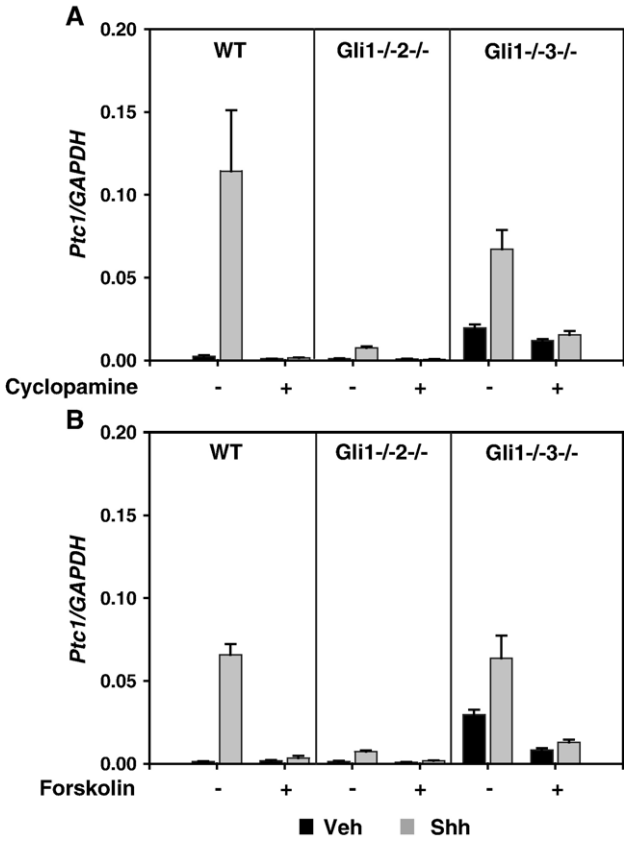

Fig. 8 – Gli2 and Gli3 exhibit common regulatory mechanisms. WT, *Gli1*$^{-/-}$*2*$^{-/-}$, and *Gli1*$^{-/-}$*3*$^{-/-}$ MEFs were plated at confluence and treated ± 10 μg/ml Shh-N, ±5 μM cyclopamine (A), or ±50 μM forskolin (B). After 48 h, expression of *Ptc1* was determined by real-time RT-PCR. Values represent the mean ± SEM of three replicate experiments.

been demonstrated to be integral in ligand-dependent antagonism of the pathway; possibly by acting as a decoy receptor for Hh ligands [41,42]. Together, Ptc1 and Hip1 are thought to function in a negative feedback loop that regulates the spatial range of Hh signaling. We speculate that the sequential induction of *Gli1*, then *Hip1* creates a temporal window of heightened responsiveness to the Hh ligand.

It is unclear whether overexpression of Gli1, a common marker of Hh-related cancers, is a significant factor in tumor biology or simply a readout of activated Hh signaling, especially given the dispensability of Gli1 but not Gli2 in normal murine development. In this study, the loss of *Gli1* by itself had no effect on target gene induction but an effect was seen when *Gli1* was lost in combination with *Gli2* or *Gli3*. The diminished capacity of cells lacking *Gli2* to induce *Ptc1* and *Hip1* was exacerbated by the additional loss of *Gli1* (Fig. 2B). Similarly, loss of *Gli3* elevated basal and Shh-induced *Ptc1* and *Hip1* expression, whereas cells lacking both *Gli3* and *Gli1* exhibited increased basal but not Shh-induced target gene expression (Fig. 3B). These observations support the previously advanced notion of a functional redundancy or cooperativity between Gli2 and Gli1 in activation of target genes [18,43] and indicate a functional cooperation between Gli3 and Gli1. However, our observations further establish that Gli1 can function as a transcriptional activator in the absence of Gli2 and Gli3 (Fig. 6). These results contrast with the findings of Buttitta et al. [11] who found that *Gli1* overexpression could not transcriptionally activate downstream targets *Ptc1* and *Hip1* in cultured presomitic mesoderm tissue from *Gli2*$^{-/-}$*3*$^{-/-}$ mice. The best explanation for this discrepancy is differences in the specific properties of the presomitic mesoderm and the MEF cell based system. The capacity of Gli1 to mediate target gene activation both in the presence or absence of Gli2 and/or Gli3 is of particular relevance to the role of Hh pathway activation in cancer, as *Gli1* overexpression is a consistent hallmark of tumors associated with aberrant Hh signaling.

Infection of WT MEFs with Gli1-GFP encoding adenovirus caused an increase in *Gli1* expression comparable to stimulation by Shh peptide (Fig. 6). However, the overexpression of *Gli1* alone caused only a minimal increase in *Ptc1* and *Hip1* induction compared to Shh stimulation. This indicates that the increased *Gli1* expression following Shh stimulation is not the primary mediator of *Ptc1* and *Hip1* induction.

While we found that *Gli1* was not the primary positive mediator of Hh target gene expression, our studies show that Gli2 plays the preeminent role in the transcriptional activation response to Hh signaling. We found that Shh stimulation induced *Ptc1* and *Hip1* expression in *Gli1*$^{-/-}$*3*$^{-/-}$ MEFs, establishing that Gli2 transactivation capacity requires neither Gli1 nor Gli3, and also found a gene-dose dependent effect of *Gli2* loss of function on target gene activation that reveals functional haploinsufficiency at the cellular level. The impaired induction of *Gli1* expression in *Gli2*$^{-/-}$ MEFs is consistent with the observed reduction of *Gli1* expression in the *Gli2* null mouse [12,13] and with recent work showing that Gli2 directly regulates *Gli1* expression by binding to the *Gli1* promoter [44]. Some studies examining the role of Gli2 in developmental contexts have suggested that it can function as a Hh target gene repressor [11,15]. We found no evidence for a role of Gli2 as a repressor of the target genes we assayed. Neither *Gli2*$^{-/-}$ nor *Gli1*$^{-/-}$*2*$^{-/-}$ MEFs exhibited elevated basal or Shh-induced levels of target gene expression (Fig. 2A). Taken together, our findings do not provide any data in support of the postulated role of Gli2 as a repressor of Hh target gene expression. However, our study focused on the conserved target genes *Gli1*, *Ptc1*, and *Hip1* and it is possible that Gli2 could repress other target genes not studied here.

Our studies verified that Gli3 acts primarily as a transcriptional repressor and found that repression activity to be independent of the activity of Gli1 or Gli2. Gli3 may also enable an increase in target gene expression but it remains unclear whether this is a direct transactivating effect or a secondary effect achieved through Gli1 and/or Gli2. Shh stimulation significantly induced *Ptc1* and *Hip1* expression in *Gli1*$^{-/-}$*2*$^{-/-}$ MEFs, a finding that suggests that Gli3 can directly regulate their expression. To distinguish Shh-induced transactivation by Gli3 from Shh-induced relief of repression by Gli3, we compared the level of Shh-induced target gene expression in MEFs expressing only *Gli3* to the basal level of expression in MEFs expressing only *Gli1* or *Gli2*. Shh-induced target gene expression in MEFs expressing only *Gli3* that exceeded the basal levels of expression in *Gli1*$^{-/-}$*3*$^{-/-}$ or *Gli2*$^{-/-}$*3*$^{-/-}$ MEFs would indicate a clear transactivation capacity for Gli3. However, we

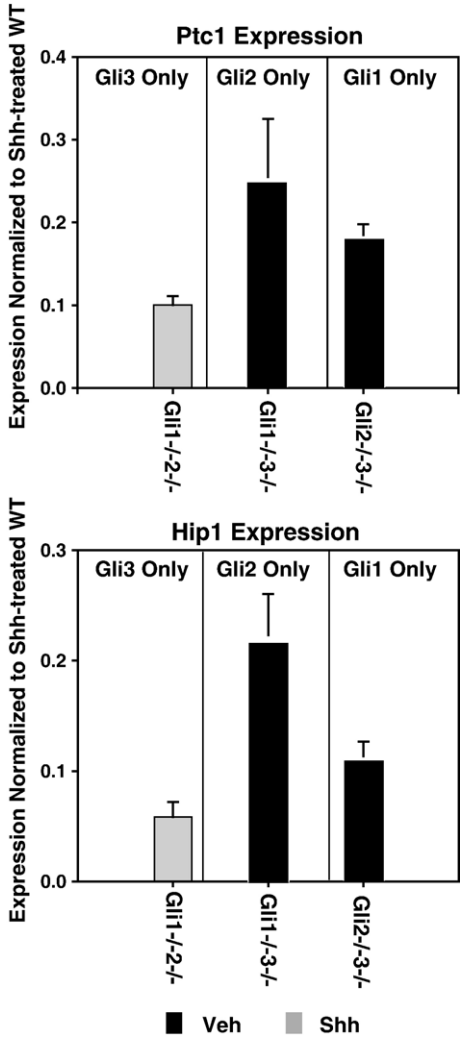

Fig. 9 – Shh-induced target gene expression in MEFs expressing only *Gli3* does not exceed basal expression in MEFs lacking Gli3. Shh-induced *Ptc1* and *Hip1* expression in *Gli1*$^{-/-}$*2*$^{-/-}$ MEFs and the basal *Ptc1* and *Hip1* expression levels in *Gli1*$^{-/-}$*3*$^{-/-}$ and *Gli2*$^{-/-}$*3*$^{-/-}$ MEFs were normalized to the Shh-induced expression levels in respective WT MEFs.

found that Shh-induced *Ptc1* and *Hip1* expression in *Gli1*$^{-/-}$2$^{-/-}$ MEFs never exceeded the basal levels of expression in either *Gli1*$^{-/-}$3$^{-/-}$ or *Gli2*$^{-/-}$3$^{-/-}$ MEFs (Fig. 9). This leaves open the possibility that the Shh-stimulated increase in target gene expression in MEFs expressing only *Gli3* reflects only the reversal of Gli3 repressor activity. Significantly, elevated basal levels of expression were seen in *Gli1*$^{-/-}$3$^{-/-}$ (Fig. 3A) and *Gli2*$^{-/-}$3$^{-/-}$ MEFs showing that the increase in basal target gene expression can occur in the absence of either Gli1 or Gli2. However, target gene activation did not occur in the combined absence of Gli2 and Gli3. Taken together, these observations suggest that Gli3 plays a key role in repressing target gene expression in the basal state and contributes to target gene activation at least by a direct derepression and possibly by direct transcriptional activation (summarized in Fig. 10). In the absence of Hh ligand, Gli3 represses Gli1- and Gli2-mediated target gene activation. This is supported by the observation that *Gli1* overexpression resulted in higher expression levels of both *Ptc1* and *Hip1* in *Gli2*$^{-/-}$3$^{-/-}$ MEFs compared to WT MEFs (Fig. 6; $P = 0.0016$ and $P = 0.012$, respectively, paired *t* test).

Hh ligand binding is thought to induce activation of Gli2 mediated transcriptional activity. Since the induction of target genes is reduced in *Gli2*$^{-/-}$ MEFs, we infer that Gli2 mediates the normal increase in their expression. Because the basal level of target gene expression is increased in *Gli3*$^{-/-}$ MEFs, we also infer that Gli3 acts to repress basal expression. Thus, it is likely that Shh stimulation initially increases target gene expression by two mechanisms: by activating Gli2 as a positive regulator of expression and by relieving the repressive function of Gli3. Like *Ptc1* and *Hip1*, *Gli1* expression is regulated by Gli2 and Gli3 and it can mediate target gene activation in the absence of Gli2 or Gli3. With the combined loss of Gli3 and Gli2, basal target gene expression is de-repressed but cannot be further upregulated by Gli2 in response to Hh ligand.

Several studies suggest that Gli2 is a potent activator of Hh target genes, that Gli1 is a weaker activator that provides functional redundancy for Gli2 and that Gli3 possesses at most a weak capacity for gene transactivation [9,43,44]. All three Gli proteins bind to a consensus promoter sequence [46], but it is not known to what extent, if any, the different Gli proteins may exhibit differential affinity for various binding sites. It is also not known whether the relative weak transactivating capabilities of Gli1 and Gli3 allow them to function in varying capacities and in different circumstances to augment the activating function of Gli2 or to act as competitive partial antagonists.

In *Drosophila*, Ci acts as both a repressor and activator of Hh target genes. This bimodal activity depends upon a complex network of regulatory elements that is modulated by Hh stimulation. Considerable uncertainty exists as to whether Gli2 and Gli3 have evolutionarily conserved regulatory mechanisms from their Ci ancestor.

We found that the induction of *Ptc1* through both Gli2 and Gli3 was blocked by cyclopamine (Fig. 8A), which has been shown to block Hh signaling by directly binding the heptahelical bundle of Smoothened (Smo) [45]. Therefore, our findings provide initial evidence that, in vertebrates, Hh signaling acts through Smo to regulate the activity of both Gli2 and Gli3.

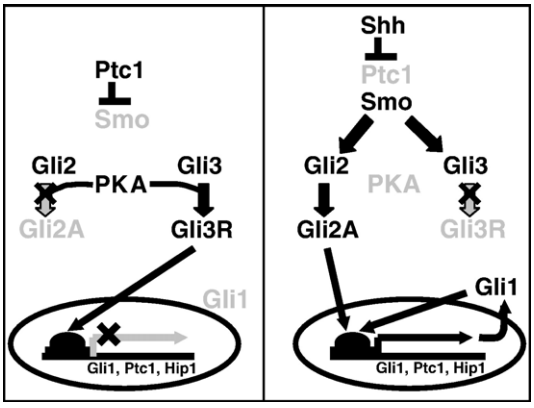

Fig. 10 – Upstream regulation of the Gli transcription factors and their individual and combinatorial roles in regulating Hh target gene expression.

The formation of the repressor form of Ci requires phosphorylation of specific serine–threonine residues by PKA [39], which is thought to promote the subsequent cleavage of Ci to generate the repressor form. We found that forskolin, an activator of adenylate cyclase, inhibited both Gli2- and Gli3-mediated Hh target gene induction. Like Ci, both Gli3 and Gli2 have PKA site clusters C-terminal to the zinc finger [6] and a PKA-dependent phosphorylation and subsequent cleavage generating a Gli3 repressor form have been described [6]. Similarly, Wang et al. found that activation of PKA by forskolin resulted in phosphorylation of Gli2 but did not generate a cleavage product. Our findings suggest that indeed regulation by PKA is a conserved mechanism of upstream regulation for Gli2 and Gli3.

While these MEF-based assays cannot account for possible tissue specificity of Gli function, taken together this quantitative, cellular level analysis of Gli function largely correlates with the various tissue level analysis of *Gli* mutant mice [9,11,12,18,26] as well as to our analysis of Gli function in tissue-specific urogenital sinus mesenchymal cells. Furthermore, unlike previous reports examining Hh signaling in Gli null mouse models, this study demonstrates that the effects of Gli2 and Gli3 LOF on Hh signaling are due to dynamic loss of Gli function and not from fixed compensatory mechanisms and/or other secondary effects of chronic Gli loss of function. The model presented here (Fig. 10) is in agreement with the model presented by Bai et al. [9], but also includes some upstream regulators of Gli2 and Gli3 and ascribes independent actions of each Gli in the overall regulation of Hh target gene transcription.

In the absence of Hh ligand, Ptc1 suppresses Smo activity. Based upon data presented here and findings in other systems, we postulate that this suppression, along with additional negative regulation involving PKA activity, stifles Gli2 activation and promotes the processing of Gli3, generating a repressor form which blocks Hh target gene transcription. Upon stimulation by Hh ligand, the Ptc1 mediated suppression of Smo is relieved, which concurrently relieves the processing of Gli3 and promotes the activation of Gli2. The combination of Gli2 activation and loss of Gli3 repression results in the transcription of Hh target genes including *Gli1*, which in specific contexts can then further drive target gene expression. Significantly, in this model, Gli2 and Gli3 share common upstream control mechanisms but act independently of each other to regulate target gene transcription. Furthermore, while Gli1 expression is regulated by Gli2 and Gli3 activity, it requires neither Gli2 nor Gli3 to induce target genes. Additionally, our finding that Shh stimulation does not modulate the induction of target genes by Gli1 overexpression in $Gli2^{-/-}3^{-/-}$ MEFs suggests that Shh regulates Gli1 through transcriptional regulation via Gli2 and Gli3 and not at the post-transcriptional level.

This study aimed to describe the roles of the Gli transcription factors in a general context that could be extrapolated to the study of Hh signaling in its many critical biological contexts and indeed has relevance to the recently recognized role of the *Gli* genes in human teratology and tumor biology. In the human population, a set of related birth defects termed holoprosencephaly is linked to perturbed Hh signaling during development (reviewed in [47]). Genetic studies of affected humans have in fact revealed a significant incidence of single allele mutations in *Shh* and *Gli2* [48,49], but linkage studies of familial cases show variable and incomplete penetrance, a finding that has led to speculation that environmental influences may interact with genetic mutations. Our studies demonstrate a heretofore unknown haploinsufficiency in *Gli2* function which may prove critical in lowering the threshold of sensitivity to environmental or dietary Hh signaling inhibitors.

Hh pathway activation has been implicated in a variety of childhood and adult tumors, including medulloblastoma, basal cell carcinoma, small cell lung cancer, and pancreatic and prostate cancer (reviewed in [22]). Analysis of *Gli* gene expression among relevant tumor tissue samples and tumor cell lines show an inconsistent pattern of *Gli* gene expression, with some expressing only a subset of *Gli* genes [20,50]. Understanding the specific activities of each of the three *Gli* genes in the canonical response to Hh signaling, as described here, will provide a basis upon which to formulate specific mechanistic studies of the role of the specific Gli genes in Hh pathway activation in human tumors.

Acknowledgments

We thank Alexandra Joyner for providing Gli1 and Gli2 transgenic mice and Laura Buttitta and Chen-Ming Fan for providing GFP, Gli-GFP, Gli2-GFP, and Gli3-GFP adenoviral constructs. We also thank Dave Walterhouse, Robert Holmgren, and Aubie Shaw for critical review of the manuscript and John Fallon, Sean Hasso, Warren Heideman, and Chimera Peet for helpful suggestions. We also thank Alejandro Munoz del Rio, Norman Drinkwater, and Michael Newton for assistance with statistical analysis. This work was supported by grants from the National Institute of Health (DK 52689 and DK 56238). R.J.L. was supported by a Molecular and Environmental Toxicology Training Grant from the National Institute for Environmental Health Sciences (T32-ES07015) and J.Z. was supported in part by a grant from the Department of Defense (W81XWH-04-1-0157). Contribution 376, Molecular and Environmental Toxicology Center, University of Wisconsin-Madison, Madison, WI 53726.

REFERENCES

[1] P.W. Ingham, A.P. McMahon, Hedgehog signaling in animal development: paradigms and principles, Genes Dev. 15 (2001) 3059–3087.
[2] M.M. Cohen Jr., The hedgehog signaling network, Am. J. Med. Genet. 123A (2003) 5–28.
[3] J. Briscoe, P. Therond, Hedgehog signaling: from the *Drosophila* cuticle to anti-cancer drugs, Dev. Cell 8 (2005) 143–151.
[4] L. Lum, P.A. Beachy, The Hedgehog response network: sensors, switches, and routers, Science 304 (2004) 1755–1759.
[5] P. Dai, H. Akimaru, Y. Tanaka, T. Maekawa, M. Nakafuku, S. Ishii, Sonic Hedgehog-induced activation of the Gli1 promoter is mediated by GLI3, J. Biol. Chem. 274 (1999) 8143–8152.
[6] B. Wang, J.F. Fallon, P.A. Beachy, Hedgehog-regulated

processing of Gli3 produces an anterior/posterior repressor gradient in the developing vertebrate limb, Cell 100 (2000) 423–434.
[7] P. Aza-Blanc, H.Y. Lin, A. Ruiz i Altaba, T.B. Kornberg, Expression of the vertebrate Gli proteins in *Drosophila* reveals a distribution of activator and repressor activities, Development 127 (2000) 4293–4301.
[8] H. Sasaki, Y. Nishizaki, C. Hui, M. Nakafuku, H. Kondoh, Regulation of Gli2 and Gli3 activities by an amino-terminal repression domain: implication of Gli2 and Gli3 as primary mediators of Shh signaling, Development 126 (1999) 3915–3924.
[9] C.B. Bai, D. Stephen, A.L. Joyner, All mouse ventral spinal cord patterning by hedgehog is Gli dependent and involves an activator function of Gli3, Dev. Cell 6 (2004) 103–115.
[10] Q. Lei, A.K. Zelman, E. Kuang, S. Li, M.P. Matise, Transduction of graded Hedgehog signaling by a combination of Gli2 and Gli3 activator functions in the developing spinal cord, Development 131 (2004) 3593–3604.
[11] L. Buttitta, R. Mo, C.C. Hui, C.M. Fan, Interplays of Gli2 and Gli3 and their requirement in mediating Shh-dependent sclerotome induction, Development 130 (2003) 6233–6243.
[12] Q. Ding, J. Motoyama, S. Gasca, R. Mo, H. Sasaki, J. Rossant, C.C. Hui, Diminished Sonic hedgehog signaling and lack of floor plate differentiation in Gli2 mutant mice, Development 125 (1998) 2533–2543.
[13] M.P. Matise, D.J. Epstein, H.L. Park, K.A. Platt, A.L. Joyner, Gli2 is required for induction of floor plate and adjacent cells, but not most ventral neurons in the mouse central nervous system, Development 125 (1998) 2759–2770.
[14] Ruiz i Altaba, Gli proteins encode context-dependent positive and negative functions: implications for development and disease, Development 126 (1999) 3205–3216.
[15] H. Sasaki, C. Hui, M. Nakafuku, H. Kondoh, A binding site for Gli proteins is essential for HNF-3beta floor plate enhancer activity in transgenics and can respond to Shh in vitro, Development 124 (1997) 1313–1322.
[16] C. Wetmore, Sonic hedgehog in normal and neoplastic proliferation: insight gained from human tumors and animal models, Curr. Opin. Genet. Dev. 13 (2003) 34–42.
[17] N. Dahmane, J. Lee, P. Robins, P. Heller, A. Ruiz i Altaba, Activation of the transcription factor Gli1 and the Sonic hedgehog signalling pathway in skin tumours [erratum appears in Nature 1997 Dec 4;390 (6659):536], Nature 389 (1997) 876–881.
[18] H.L. Park, C. Bai, K.A. Platt, M.P. Matise, A. Beeghly, C.C. Hui, M. Nakashima, A.L. Joyner, Mouse Gli1 mutants are viable but have defects in SHH signaling in combination with a Gli2 mutation, Development 127 (2000) 1593–1605.
[19] R.A. Benson, J.A. Lowrey, J.R. Lamb, S.E. Howie, The Notch and Sonic hedgehog signalling pathways in immunity, Mol. Immunol. 41 (2004) 715–725.
[20] S. Karhadkar, G.S. Bova, N. Abdallah, S. Dhara, D. Gardner, A. Maitra, J.T. Isaacs, D.M. Berman, P.A. Beachy, Hedgehog signalling in prostate regeneration, neoplasia and metastasis, Nature 431 (2004) 707–712.
[21] H. Ito, H. Akiyama, C. Shigeno, K. Iyama, H. Matsuoka, T. Nakamura, Hedgehog signaling molecules in bone marrow cells at the initial stage of fracture repair, Biochem. Biophys. Res. Commun. 262 (1999) 443–451.
[22] M. Pasca di Magliano, M. Hebrok, Hedgehog signalling in cancer formation and maintenance, Nat. Rev., Cancer 3 (2003) 903–911.
[23] A. Shaw, J. Papadopoulos, C. Johnson, and W. Bushman, Isolation and characterization of an immortalized mouse urogenital sinus mesenchyme cell line, Prostate (in press).
[24] V. Marigo, R.L. Johnson, A. Vortkamp, C.J. Tabin, Sonic hedgehog differentially regulates expression of GLI and GLI3 during limb development, Dev. Biol. 180 (1996) 273–283.
[25] P.T. Chuang, A.P. McMahon, Vertebrate Hedgehog signalling modulated by induction of a Hedgehog-binding protein, Nature 397 (1999) 617–621.
[26] A. McDermott, M. Gustafsson, T. Elsam, C.C. Hui, C.P. Emerson Jr., A.G. Borycki, Gli2 and Gli3 have redundant and context-dependent function in skeletal muscle formation, Development 132 (2005) 345–357.
[27] C.A. Podlasek, D.H. Barnett, J.Q. Clemens, P.M. Bak, W. Bushman, Prostate development requires Sonic hedgehog expressed by the urogenital sinus epithelium, Dev. Biol. 209 (1999) 28–39.
[28] B.E. Wang, J. Shou, S. Ross, H. Koeppen, F.J. De Sauvage, W.Q. Gao, Inhibition of epithelial ductal branching in the prostate by sonic hedgehog is indirectly mediated by stromal cells, J. Biol. Chem. 278 (2003) 18506–18513.
[29] S.H. Freestone, P. Marker, O.C. Grace, D.C. Tomlinson, G.R. Cunha, P. Harnden, A.A. Thomson, Sonic hedgehog regulates prostatic growth and epithelial differentiation, Dev. Biol. 264 (2003) 352–362.
[30] D.M. Berman, N. Desai, X. Wang, S.S. Karhadkar, M. Reynon, C. Abate-Shen, P.A. Beachy, M.M. Shen, Roles for Hedgehog signaling in androgen production and prostate ductal morphogenesis, Dev. Biol. 267 (2004) 387–398.
[31] M.L. Lamm, W.S. Catbagan, R.J. Laciak, D.H. Barnett, C.M. Hebner, W. Gaffield, D. Walterhouse, P. Iannaccone, W. Bushman, Sonic hedgehog activates mesenchymal Gli1 expression during prostate ductal bud formation, Dev. Biol. 249 (2002) 349–366.
[32] J.P. Incardona, W. Gaffield, R.P. Kapur, H. Roelink, The teratogenic Veratrum alkaloid cyclopamine inhibits sonic hedgehog signal transduction, Development 125 (1998) 3553–3562.
[33] J.K. Chen, M.K. Cooper, B. Wang, R.K. Mann, L. Milenkovic, M.P. Scott, P.A. Beachy, J. Taipale, Effects of oncogenic mutations in Smoothened and Patched can be reversed by cyclopamine [see comment], Nature 406 (2000) 1005–1009.
[34] M.C. Hu, R. Mo, S. Bhella, C.W. Wilson, P.-T. Chuang, C.-C. Hui, N.D. Rosenblum, GLI3-dependent transcriptional repression of Gli1, Gli2 and kidney patterning genes disrupts renal morphogenesis, Development 133 (2005) 569–578.
[35] W. Li, J.T. Ohlmeyer, M.E. Lane, D. Kalderon, Function of protein kinase A in hedgehog signal transduction and *Drosophila* imaginal disc development, Cell 80 (1995) 553–562.
[36] M. Hammerschmidt, M.J. Bitgood, A.P. McMahon, Protein kinase A is a common negative regulator of Hedgehog signaling in the vertebrate embryo, Genes Dev. 10 (1996) 647–658.
[37] Y. Chen, N. Gallaher, R.H. Goodman, S.M. Smolik, Protein kinase A directly regulates the activity and proteolysis of cubitus interruptus, Proc. Natl. Acad. Sci. U. S. A. 95 (1998) 2349–2354.
[38] P. Maye, S. Becker, E. Kasameyer, N. Byrd, L. Grabel, Indian hedgehog signaling in extraembryonic endoderm and ectoderm differentiation in ES embryoid bodies, Mech. Dev. 94 (2000) 117–132.
[39] H.H. Yao, W. Whoriskey, B. Capel, Desert Hedgehog/Patched 1 signaling specifies fetal Leydig cell fate in testis organogenesis, Genes Dev. 16 (2002) 1433–1440.
[40] W.J. Ingram, C.A. Wicking, S.M. Grimmond, A.R. Forrest, B.J. Wainwright, Novel genes regulated by Sonic Hedgehog in pluripotent mesenchymal cells, Oncogene 21 (2002) 8196–8205.
[41] P.T. Chuang, T. Kawcak, A.P. McMahon, Feedback control of mammalian Hedgehog signaling by the Hedgehog-binding protein, Hip1, modulates Fgf signaling during branching morphogenesis of the lung, Genes Dev. 17 (2003) 342–347.

[42] J. Jeong, A.P. McMahon, Growth and pattern of the mammalian neural tube are governed by partially overlapping feedback activities of the hedgehog antagonists patched 1 and Hhip1, Development 132 (2005) 143–154.
[43] G. Regl, G.W. Neill, T. Eichberger, M. Kasper, M.S. Ikram, J. Koller, H. Hintner, A.G. Quinn, A.M. Frischauf, F. Aberger, Human GLI2 and GLI1 are part of a positive feedback mechanism in basal cell carcinoma, Oncogene 21 (2002) 5529–5539.
[44] M.S. Ikram, G.W. Neill, G. Regl, T. Eichberger, A.M. Frischauf, F. Aberger, A. Quinn, M. Philpott, GLI2 is expressed in normal human epidermis and BCC and induces GLI1 expression by binding to its promoter, J. Invest. Dermatol. 122 (2004) 1503–1529.
[45] J.K. Chen, J. Taipale, M.K. Cooper, P.A. Beachy, Inhibition of Hedgehog signaling by direct binding of cyclopamine to Smoothened, Genes Dev. 16 (2002) 2743–2748.
[46] M. Agren, P. Kogerman, M.I. Kleman, M. Wessling, R. Toftgard, Expression of the PTCH1 tumor suppressor gene is regulated by alternative promoters and a single functional Gli-binding site, Gene 330 (2004) 101–114.
[47] M.M. Cohen Jr., K. Shiota, Teratogenesis of holoprosencephaly, Am. J. Med. Genet. 109 (2002) 1–15.
[48] L. Nanni, J.E. Ming, M. Bocian, K. Steinhaus, D.W. Bianchi, C. Die-Smulders, A. Giannotti, K. Imaizumi, K.L. Jones, M.D. Campo, R.A. Martin, P. Meinecke, M.E. Pierpont, N.H. Robin, I.D. Young, E. Roessler, M. Muenke, The mutational spectrum of the sonic hedgehog gene in holoprosencephaly: SHH mutations cause a significant proportion of autosomal dominant holoprosencephaly, Hum. Mol. Genet. 8 (1999) 2479–2488.
[49] E. Roessler, Y.Z. Du, J.L. Mullor, E. Casas, W.P. Allen, G. Gillessen-Kaesbach, E.R. Roeder, J.E. Ming, A. Ruiz i Altaba, M. Muenke, Loss-of-function mutations in the human GLI2 gene are associated with pituitary anomalies and holoprosencephaly-like features, Proc. Natl. Acad. Sci. U. S. A. 100 (2003) 13424–13429.
[50] P. Sanchez, A.M. Hernandez, B. Stecca, A.J. Kahler, A.M. DeGueme, A. Barrett, M. Beyna, M.W. Datta, S. Datta, A. Ruiz i Altaba, Inhibition of prostate cancer proliferation by interference with SONIC HEDGEHOG-GLI1 signaling, Proc. Natl. Acad. Sci. U. S. A. 101 (2004) 12561–12566.